



Contents list available at CBIORE journal website







**International Journal of Renewable Energy Development**

Journal homepage: <https://ijred.cbiorc.id>



Research Article

# Hydrogen-rich syngas production of solid waste supercritical water gasification multi-objective process optimization

Bayu Aji Saputro<sup>a,b</sup> , Adi Surjosatyo<sup>a,b,c\*</sup> , Wanda Rulita Sari<sup>a,b</sup> , Hafif Dafiqurrohman<sup>a,b</sup> ,  
Izzuddin Al Qossam<sup>a,b</sup> , Puspa Lestari<sup>b,d</sup> 

<sup>a</sup>Department of Mechanical Engineering, Faculty of Engineering, University of Indonesia, Kampus UI Depok 16424, Indonesia

<sup>b</sup>Biomass Gasification Research Laboratory, Universitas Indonesia, Kampus UI Depok 16424, Indonesia

<sup>c</sup>Tropical Renewable Energy Research Center, Faculty of Engineering, University of Indonesia, Kampus UI Depok 16424, Indonesia

<sup>d</sup>Department of Energy System Engineering, Faculty of Engineering, University of Indonesia, Kampus UI Depok 16424, Indonesia

**Abstract.** The increasing population and changing lifestyles have led to significant solid waste accumulation, necessitating efficient waste management to prevent environmental and health issues. Supercritical water gasification (SCWG) is an effective method for converting high-moisture biomass into hydrogen-rich syngas, operating at temperatures above 374°C and pressures above 490MPa. The objective of this study was to develop and validate an integrated modeling and multi-objective optimization framework, combining Response Surface Methodology (RSM), Artificial Neural Networks (ANN), and Multi-Objective Genetic Algorithm (MOGA) to maximize hydrogen-rich syngas production from municipal solid waste through SCWG. The research models and predicts the effects of feed concentration, residence time, and reaction temperature on hydrogen yield, lower heating value (LHV), and gas yield. The integrated RSM and ANN models demonstrated high predictive accuracy with  $R^2$  values exceeding 0.95. Optimization results from MOGA identified optimal parameters: a feed concentration of 2%, a reaction temperature between 490-495°C, and a residence time of 80 minutes. These conditions achieved  $H_2$  selectivity of 84.73%, an LHV of 6.95 MJ/Nm<sup>3</sup>, and a gas yield of 29.7%. The findings highlight the dominant influence of reaction temperature and residence time on hydrogen production, while feed concentration requires careful balance for optimal syngas quality. This study demonstrates that the combined use of RSM, ANN, and MOGA provides an effective framework for optimizing SCWG processes, offering practical insights for industrial-scale applications. Future research should explore additional variables such as biomass composition, pressure, and catalysts to enhance the efficiency and sustainability of hydrogen production from solid waste, supporting SCWG as a viable technology for sustainable energy production and effective waste management.

**Keywords:** Supercritical Water Gasification (SCWG), Hydrogen-Rich Syngas, Waste-to-Energy (WTE), Response Surface Methodology (RSM), Multi-Objective Optimization (MOGA)



@ The author(s). Published by CBIORE. This is an open access article under the CC BY-SA license (<http://creativecommons.org/licenses/by-sa/4.0/>).

Received: 15<sup>th</sup> Nov 2024; Revised: 16<sup>th</sup> March 2025; Accepted: 30<sup>th</sup> April 2025 Available online: 8<sup>th</sup> May 2025

## 1. Introduction

The continuously increasing population and the shift towards an instant lifestyle have significantly accelerated the accumulation of solid waste (Mondal, 2022). According to 2023 data from the Indonesia's National Waste Management Information System (SIPSN), 18.03 million tons of waste were produced, with 53.3% consisting of organic waste (Kemeterian LHK, 2023). Effective waste management is imperative to prevent the myriad health and environmental issues associated with waste accumulation (Ziraba *et al.*, 2016). Although various strategies, such as: waste reduction, recycling, thermal treatment, and landfilling have been implemented (Demirbas, 2011). However, 65.83% of waste in Indonesia is still transported to and disposed of in landfills, leading to greenhouse emissions including CO<sub>2</sub>, CH<sub>4</sub>, and N<sub>2</sub>O (Blair & Mataraarachchi, 2021; Kemeterian LHK, 2023).

Rather than modifying the landfill process, waste-to-energy (WTE) technology offers an alternative solution to reduce the

continuously increasing amount of waste (Sesotyo *et al.*, 2019). Among the various WTE technologies, direct waste incineration is the most widely used (Lombardi *et al.*, 2015). However, direct incineration for heat and electricity production has significant drawbacks, including air emissions, the production of fly ash, and the generation of corrosive gases (Lu *et al.*, 2019). Additionally, the high moisture content in organic waste (80%-90%), poses a challenge in the incineration process (Guo & Dai, 2017). Whereas supercritical water gasification (SCWG) is a more efficient thermochemical process for converting solid waste into hydrogen, particularly for waste with high moisture content, without the need for a drying process (Reddy *et al.*, 2014). SCWG operates at temperatures above 374°C and pressures above 22.1 MPa, where water exhibits unique properties such as a low dielectric constant, high diffusivity, and enhanced reactivity (Brunner, 2009; Hantoko *et al.*, 2019; Jin *et al.*, 2015; Kulkarni *et al.*, 2023). These condition favor rapid and efficient decomposition of long-chain molecules found in biomass, such as lignin, cellulose, proteins, and lipids, are

\* Corresponding author

Email: [adi.surjosatyo@ui.ac.id](mailto:adi.surjosatyo@ui.ac.id); [adisur@eng.ui.ac.id](mailto:adisur@eng.ui.ac.id) (A.Surjosatyo)

hydrolyzed into products like phenols, glucose, and fatty acids into gaseous products including H<sub>2</sub>, CO, CH<sub>4</sub>, and CO<sub>2</sub> (Rodriguez Correa & Kruse, 2018).

The performance of SCWG process is influenced by several factors, including reactor type, heating rate, residence time, pressure, reaction temperature, catalyst, and feed concentration (Basu & Mettanan, 2009). Studies have investigated the effects of feed concentration, residence time, and reaction temperature on hydrogen production, lower heating value (LHV), and gas yield (Khandelwal et al 2024; Nanda et al. 2018; Yan et al. 2019). The yield of hydrogen-rich syngas significantly influenced by these variables, with Increased residence time and reaction temperature generally enhancing hydrogen production, whereas higher feed concentration typically leads to its reduction (Nanda et al, 2018; Su et al., 2020; Su et al., 2020).

Statistical approaches such as Response Surface Methodology (RSM) have been widely utilized to develop empirical models that describe the relationship between key process parameters and response variables (Bakari et al., 2021; Zandifar et al., 2024). RSM enables the identification of optimal operating conditions by systematically evaluating the combined effects of variables such as feed concentration, residence time, and reaction temperature (Houcinate et al. 2018). In addition, Artificial Intelligence (AI)-based modeling approach, such as Artificial Neural Networks (ANN) have been increasingly employed to model complex gasification systems due to their ability to capture nonlinear interactions and reduce experimental costs (Evans, 2019; Rizal et al., 2024). Furthermore, AI techniques can be utilized to develop predictive models that's forecast hydrogen content in syngas based on variations in feed concentration, residence time, and reaction temperature, thereby enabling more efficient process optimization (Li et al., 2021).

Numerous studies have explored the optimization of SCWG using statistical, machine learning (ML), and metaheuristic approaches. Albarelli et al. (2017) performed a multi-objective optimization of SCWG focusing on energy efficiency, economic viability, and environmental impact (Albarelli et al. 2017). Houcinat et al. (2018) developed a kinetic model and applied Response Surface Methodology (RSM) to optimize gas yields and energy efficiency from supercritical glycerol gasification (Houcinate et al., 2018). Bakari et al. (2021) conducted parametric optimization of rice husk SCWG using the I-optimality design in RSM and found temperature to be the most significant factor affecting GE and gas yield (Bakari et al., 2021). Li et al. (2021) further demonstrated that ANN alone can predict SCWG outcomes with high accuracy, particularly in catalyst screening and hydrogen yield optimization (Li et al., 2021). Shen et al. (2025) applied MCDM to evaluate feedstock and process alternatives in plastic waste SCWG (Shen et al., 2025). Aentung et al. (2024) combined RSM with Genetic Algorithms to reduce tar in co-gasification (Aentung et al., 2024). Qiao et al. (2024) used PSO and regression for optimizing hybrid gasification-SOFC systems (Qiao et al., 2024).

To the best of our knowledge, no previous study has systematically integrated Response Surface Methodology (RSM), Artificial Neural Network (ANN), Multi-Objective Genetic Algorithm (MOGA), and Multi-Objective Ant Lion Optimizer (MOALO) into a unified modeling and optimization

framework for the supercritical water gasification (SCWG) of municipal solid waste. While numerous studies have independently employed RSM or ANN for parametric modeling, and others have applied metaheuristic algorithms such as Genetic Algorithm (GA) or Particle Swarm Optimization (PSO) for process optimization, none have combined these four techniques to concurrently model, predict, and optimize critical performance indicators in SCWG. This study, therefore, addresses a notable research gap by proposing a hybrid, multi-level framework that integrates experimental design, nonlinear predictive modeling, global optimization, and decision-support analysis.

In this research, feed concentration, residence time, and reaction temperature are selected as key input variables, while hydrogen content, gas yield, and LHV serve as the main performance targets. The framework begins by constructing data-driven predictive models using RSM and ANN to capture both linear and nonlinear relationships within the process. These models are subsequently coupled with MOGA and MOALO to explore and identify optimal input combinations that maximize the selected performance criteria. The resulting Pareto-optimal solutions are visualized through Pareto fronts, enabling a clear representation of trade-offs among competing objectives. For final decision-making, the Technique for Order Preference by Similarity to Ideal Solution (TOPSIS) is employed to rank the optimal solutions based on proximity to the ideal outcome. This integrated approach enables accurate prediction and efficient multi-objective optimization of SCWG performance. By combining modeling, optimization, and decision-making in a single framework, the study provides a practical tool for evaluating trade-offs and improving process design in waste-to-energy conversion systems. Therefore, the objective of this study is to systematically optimize hydrogen-rich syngas production from municipal solid waste using SCWG by integrating modeling tools such as RSM, ANN, and metaheuristic algorithms like MOGA and MOALO.

2. Methodology

2.1 Data Collection

The dataset for the development of the optimization model is obtained from experimental studies conducted by (Yan et al., 2019) and (Khandelwal et al., 2024) using food and agricultural waste. A total of 25 datasets (150 data points) were obtained, representing the main parameters of the supercritical water gasification process, with feed concentration ranging from 2wt% to 25wt%, residence time from 20 minutes to 80 minutes, and reaction temperature from 350°C to 500°C. The gasification results include LHV (1.15 MJ/Nm<sup>3</sup> to 6.83 MJ/Nm<sup>3</sup>), gas yield (8.13% to 29.7%), and hydrogen content in the syngas (20.3% to 89.33%). The obtained dataset was then categorized into input data (feed concentration, residence time, reaction temperature) and output/target data (LHV, gas yield, H<sub>2</sub> Selectivity) and used to develop the predictive data model.

2.2 Characterization of feedstock and SCWG products

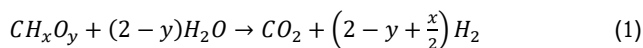
In this research, the biomass used includes food and agricultural waste. The characteristics of the syngas were

Table 1  
The Chemical Properties of the Biomass

	C	H	N	S	O	LHV	HHV
Food Waste	48.12	7.02	3.73	0.78	39.13	21.38	n.a
Agricultural Waste	46.3	6.8	0.9	0.4	45.6	n.a	18.9

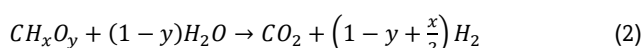
obtained through experimental studies conducted by (Yan *et al.*, 2019) and (Khandelwal *et al.*, 2024). The biomass content was tested using ultimate analysis, and the test results are shown in Table 1.

In general, the chemical reaction that occurs in supercritical water gasification to produce hydrogen gas can be expressed by a simplified reaction (Guo *et al.*, 2007) as shown in Equation (1).



In addition to the general reaction described earlier, there are three other reactions that occur during the supercritical water gasification process, which are:

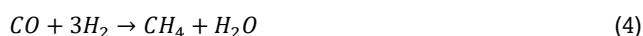
Steam reforming:



Water-gas shift:



Methanation:



The product gas generated from supercritical water gasification is then analyzed using gas chromatography. To evaluate the efficiency of SCWG, several parameters within the syngas, such as LHV, gas yield, and H<sub>2</sub> Selectivity, need to be assessed. Gas yield, H<sub>2</sub> Selectivity, and LHV can be determined using the following equations (6), (7), and (8).

$$\text{Syngas yield} \left( \frac{\text{mol}}{\text{kg}} \right) = \frac{\text{moles of gas produced}}{\text{total mass of biomass}} \quad (6)$$

$$H_2 \text{ Selectivity} (\%) = \frac{\text{moles of Hydrogen}}{\text{moles of CO, CH}_4, \text{ and CO}_2} \quad (7)$$

$$\text{Syngas yield} \left( \frac{\text{MJ}}{\text{kg}} \right) = H_2 \text{ yield} \times LHV_{H_2} + CO \text{ yield} \times LHV_{CO} + CH_4 \text{ yield} \times LHV_{CH_4} \quad (8)$$

### 2.3 RSM-Based Predictive Model

Design of Experiment (DoE) plays a crucial role in the development, improvement, and optimization of processes. The principles of statistical sampling in DoE methods are applied to achieve desired outcomes with a minimal number of experiments. By using statistical methods, DoE can study and determine cause-effect relationships, interactions, and dependencies among different experimental parameters. (Durakovic, 2017). The DoE method also allows for the simultaneous study of multiple factors and the evaluation of interaction effects, based on a two-level factorial design. Response Surface Methodology (RSM) is one of the statistical techniques frequently used in DoE to develop predictive models and optimize processes. RSM utilizes mathematical functions to construct a response surface that describes the relationship between several input variables and the desired response (Inayat *et al.*, 2020). RSM combines regression models, separate model coefficients, and deficiency of fit. The significance of the RSM model coefficients can be evaluated using analysis of variance (ANOVA), where the F-value indicates the comparison

of variance between groups and within groups, and the p-value indicates the probability of obtaining more accurate data (Fozar *et al.*, 2019; Shahbaz *et al.*, 2017). RSM combines regression models, separate model coefficients, and deficiency of fit. The significance of the RSM model coefficients can be evaluated using analysis of variance (ANOVA), where the F-value indicates the comparison of variance between groups and within groups, and the p-value indicates the probability of obtaining more accurate data (Okolie *et al.*, 2020; Zaman *et al.*, 2020). Through this approach, RSM can determine optimal conditions by maximizing or minimizing a specific response.

In this study, the RSM approach was conducted using Design Expert version 13.0.5.0. Data obtained from previous experimental studies were utilized in the modelling and optimization of SCWG. Input parameters such as feed concentration, residence time, and reaction temperature, which influence the SCWG process, were operated within minimum (-1) and maximum (1) ranges to produce optimal output variables (LHV, gas yield, and H<sub>2</sub> Selectivity to obtain maximum and saddle values in the RSM optimization process, a general polynomial equation with a quadratic model in Equation (9) can be used.

$$Y = \beta_0 + \sum_{i=1}^k \beta_i X_i + \sum_{i=1}^k \beta_{ii} X_i^2 + \sum_{i=1}^k \sum_{j=1}^k \beta_{ij} X_i X_j + \epsilon \quad (9)$$

Where Y is the measured response,  $\beta_0$  is the intercept (constant),  $\beta_i$  is the linear coefficient for factor  $X_i$ ,  $\beta_{ii}$  is the quadratic coefficient for factor  $X_i$ , and  $\beta_{ij}$  is the interaction coefficient between factors  $X_i$  and  $X_j$ .  $X_i$  and  $X_j$  are the input variables (factors) being studied, k is the number of variables, and  $\epsilon$  is the error term. The components of this equation are related as follows:

- $\beta_0$  : The intercept or constant value, representing the average response when all independent variables  $X_i$  are zero.
- $\beta_i X_i$  : The linear component, which describes the change in response Y due to the change in factor  $X_i$ .
- $\beta_{ii} X_i^2$  : The quadratic component, which describes the non-linear effect of factor  $X_i$  on response Y.
- $\beta_{ij} X_i X_j$  : The interaction component, which describes the combined effect of two factors  $X_i$  and  $X_j$  on response Y.

To estimate the parameters in Equation (9), data obtained from previous experimental studies must ensure that each investigated variable is conducted at least three levels of factors.

### 2.4 ANN-Based Predictive Model

Artificial Neural Network (ANN) is a computational technique developed based on the biological neural network process, which is inspired by natural neurons and mimics the behavior and learning processes of the human brain. (Pandey *et al.*, 2016). ANN consists of neurons or nodes as processing elements that are interconnected and work together to solve specific problems. These neurons are grouped into different layers and interconnected according to a particular architecture. Each layer has weight matrices, bias vectors, and output vectors (Puig-Arnavat *et al.*, 2013). This method can be utilized for response variable values with one or more working factor variables (Ascher *et al.*, 2022).

In this study, a Multilayer Perceptron (MLP) model with a feed-forward configuration of an Artificial Neural Network (ANN) was developed, as shown in Figure 1. The utilization of the MLP model is effective in estimating the functional structure in nonlinear systems and can be applied to various problems such as classification and regression (Du *et al.*, 2022). The MLP

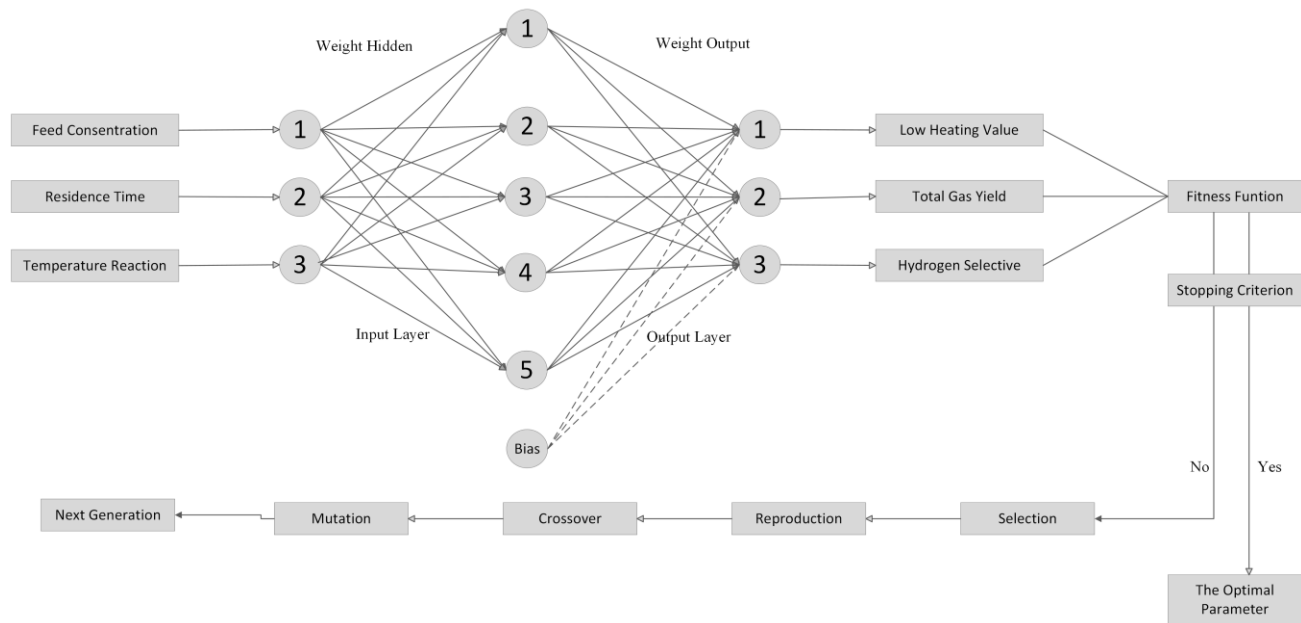


Fig. 1 Development Architect of ANN

structure involves multiple layers, including the input layer, hidden layers, and output layer in a feed-forward manner. In this model, the number of hidden layers can affect the convergence and performance of the neurons (Kiranyaz *et al.*, 2017; Lin *et al.*, 2024). Behind each hidden layer and output layer, there is a bias value ( $b$ ) associated with the weight parameters ( $w$ ) used for network development. The optimal network size depends on the number of neurons in the output layer, which is determined through a trial-and-error process with a heuristic approach. Developing the appropriate number of neurons is crucial, as having too many or too few can lead to overfitting or underfitting of the results (Rizal *et al.*, 2024). The computation of the predicted output from the ANN model follows the weighted activation function described in Equation (10) (Ascher *et al.*, 2022).

$$y_k = f_0(\sum_h w_{hk} f_h(\sum_i w_{ih} x_i)) \quad (10)$$

Where the value  $y_k$  represents the network's prediction of the response. This prediction is calculated from the sum of the products of the weights ( $w$ ) and input variable ( $x$ ) for each hidden layer ( $h$ ). This product is then passed through the activation function  $f_0$  for the output node and  $f_h$  hidden node (Beck, 2018).

In this study, training data with a backpropagation model with 1000 epochs and zero target on the ANN was performed using the Bayesian Regularization (BR) method, where an optimal weight that minimizes prediction error for the test data set is obtained through an iterative process. Training data in ANN modeling involves modifying the network by presenting input data along with the desired output. During the training process, the weights within the network are adjusted to achieve results that approximate the target output (desired output), where the weights after training contain a significant amount of information (Kayri, 2016).

In this study, 75% of the experimental dataset was used for training the neurons, and 25% of the dataset was used for validation and testing. After the experimental data was validated, it was input into the model under various input conditions. The neuron training process aids in the optimal development of the ANN model through synaptic adjustments,

while the validation process focuses on the neuron's learning curve. Both processes are halted when the Mean Square Error (MSE) in training exceeds the value from the validation process. To select the best estimator during the prediction phase, we use the parameters MSE and the coefficient of determination ( $R^2$ ) within the ANN. The values of MSE and  $R^2$  can be evaluated using Equations (11) and (12).

$$MSE = \frac{1}{N} \sum_{i=1}^N (|y_{p,i} - y_{exp,i}|)^2 \quad (11)$$

$$R^2 = 1 - \frac{\sum_{i=1}^N (y_{p,i} - y_{exp,i})}{\sum_{i=1}^N (y_{p,i} - y_{av})} \quad (12)$$

where,  $y_{p,i}$  is the anticipated value of the ANN model,  $y_{exp,i}$  experimental efficiency value,  $y_{av}$  average experimental efficiency value, and proportional value of the amount of data.

## 2.5 Multi-Objective Genetic Algorithm (MOGA) Based Predictive Model

The Genetic Algorithm (GA) is frequently used to solve optimization problems by mimicking natural processes (Zhu *et al.*, 2020). In this study, the optimization technique employed is based on the Genetic Algorithm, commonly known as the Multi-Objective Genetic Algorithm (MOGA), which has been widely used in various energy optimization fields such as waste gasification, gas fractionation, and fuel cell integration (Pandey *et al.*, 2015). MOGA differs from other algorithms as it works with a group of solutions rather than solving a single problem. Based on the fitness function of MOGA, each solution from a group of solutions is evaluated based on how well the group of solutions meets multiple specified objectives. These solutions are ranked based on the number of solutions they dominate (Sun *et al.*, 2022). Based on Figure 1, the optimization process follows these steps:

1. Development of the fitness function occurs after the ANN process.
2. Selection of the initial population.
3. Determination of upper and lower bounds based on experimental data results.

4. Using the fitness function value as the individual data value, then the best individuals are used as parents for the next group.
5. Parents are evaluated and obtain information through various crossovers and mutations to generate a new group.
6. Repeat steps 1-5 until the results meet the stop criterion. In this case, iterations aim to achieve convergence to a zero value in the fitness function for each group.

Using MOGA, the optimization results are depicted in a Pareto graph, where trade-offs are evaluated to meet different objectives. In this study, multi-objective optimization is formulated based on a set of objective functions and constraints. Equation (13) defines the general form of the optimization model, while Equation (14) expresses the multi-objective function vector. The constraints applied to the model are expressed in Equation (15) for inequality constraints, and Equation (16) for equality constraints, which together define the feasible solution space for optimization.

$$\text{Find } x = (x_i) \forall i = 1, 2, \dots, N_{par} \quad (13)$$

$$\text{Minimizing or maximizing } f_i(x_i) \forall i = 1, 2, \dots, N_{obj} \quad (14)$$

$$g_j(x) = 0 \quad \forall j, 1, 2, \dots, m \quad (15)$$

$$h_k(x) = 0 \quad \forall k, 1, 2, \dots, m \quad (16)$$

Where,  $N_{par}$  is the number of decision variables,  $f_i(x_i)$  represents the objective functions,  $N_{obj}$  is the total number of objective functions,  $x$  is the vector of choice variables,  $g_j(x)$  and  $h_k(x)$  are the equality and inequality constraints, respectively.

## 2.6 Multi-objective Ant Lion Algorithm (MOALO) Based Predictive Model

MOALO is a multi-objective optimization development of ALO (Mirjalili, 2015). It is a nature-inspired metaheuristic algorithm that imitates the foraging behavior of ants and has been successfully used in various engineering optimization problems (Mirjalili *et al.*, 2017; Hardiansyah, 2021; Soesanti and Syahputra, 2022). The MOALO technique consists of five stages: random walking, building traps, inserting ants into traps, capturing prey, and rebuilding traps (Mirjalili *et al.*, 2017). In the MOALO there are two population with set of ants and sets of antlions. The general steps of the MOALO for modifying these two sets and ultimately estimating the global optimum for a given optimization problem are as follows:

1. Initial populations for both ants and antlions are set up, and the size of the archive is determined. The antlions are initially assumed to be at the positions of ants in the first iteration.
2. The fitness value of each ant is evaluated using an objective function in each iteration. The objective roles of ants and antlions are assessed.
3. The iterative process begins, using the roulette wheel approach to select the antlion and elite from the archive for each ant. Ants move through the search space using random walks around the antlions. The radius of these random walks is modified, normalized, and verified within the boundaries.
4. In subsequent iterations, antlions relocate to the new positions of ants if the ants show better fitness. Each ant is assigned to an antlion, which updates its position if the ant achieves higher fitness. An elite antlion influences the movement of all ants, regardless of their distance. If an antlion surpasses the elite in fitness, it replaces the elite.

5. The fitness of all ants is computed with the following position updates. The archive is updated and its condition verified.
6. Steps 2 through 5 are repeated until an end criterion is met.
7. The final position and fitness value of the elite antlion are returned as the best estimation for the global optimum, and the updated archive is outputted.

Multi-objective Ant Lion Optimization (MALO) offers advantages such as simplicity, scalability, and flexibility, making it suitable for practical applications in power system optimization and engineering design problems (Durgut *et al.*, 2024). By utilizing the Multi-Objective Ant Lion Optimizer (MOALO), the results yielded optimal solutions positioned along the Pareto front. This facilitated the evaluation of trade-offs to achieve multiple objectives concurrently. MOALO effectively identified the most favorable solutions by taking into account various competing factors, thereby enhancing the decision-making process.

## 2.7 Technique for Order Preference by Similarity to Ideal Solution (TOPSIS)

The Technique for Order Preference by Similarity to Ideal Solution (TOPSIS) is a prominent distance-based multi-criteria or multi-attribute decision-making (MCDM/MADM) technique (Shih, 2022). It evaluates alternatives and identifies the ideal solution by ranking a limited number of alternatives based on their closeness to an idealized goal (S. K. Yadav *et al.*, 2018). The method involves determining the Positive Ideal Solution (PIS) and Negative Ideal Solution (NIS) of the alternatives and designing different TOPSIS models according to the distance measures of each alternative to these ideal solutions (Qian *et al.*, 2023). The best alternative is selected based on its Euclidean distance from the ideal solution (V. Yadav *et al.*, 2019). In this study, TOPSIS is employed to determine the most optimal value of a SCWG process produced by both the Multi-Objective Genetic Algorithm (MOGA) and the Multi-Objective Ant Lion Optimizer (MOALO) from both the Design of Experiment (DoE) and Artificial Neural Network (ANN) models. TOPSIS was conducted using MATLAB software to ascertain the most optimal value. Firstly, the criteria values are transformed into a comparable scale through normalization. Subsequently, the normalized decision matrix is multiplied by the weights assigned to each criterion to generate the weighted normalized matrix. This matrix is then utilized to identify the optimal (positive ideal) and suboptimal (negative ideal) values for each criterion. Following this step, the Euclidean distance is computed to ascertain the distance of each alternative from both the positive ideal solution and the negative ideal solution. The proximity of each alternative to the optimal solution is then assessed. Finally, the alternatives are evaluated and ranked according to their proximity to the ideal solution, with the highest proximity indicating the most optimal choice.

## 3. Result and Discussion

### 3.1 Response Surface Methodology Model Validation

To observe the relationship between the three independent variables and the three responses from the supercritical water gasification process, modeling was conducted using Response Surface Methodology (RSM) through several development stages, including model determination, factor level setting, design selection, evaluation, validation, and optimization (Gammoudi *et al.*, 2021). The Design of Experiment (DoE) plays a crucial role in the development of the RSM model, as it enables the collection of well-distributed data according to specific constraints of the independent variables. DoE can explain the

**Table 2**  
ANOVA result of H2 selective, LHV, and Gas Yield

Response	Process Order	Source	Sum of Square	df	Mean Square	F-value	P-Value
H2 Selective	Quadratic	Model	6530.36	9	725.60	16.62	<00001
		A: Feed Concentration	933.48	1	933.48	21.38	<0.0001
		B: Residence Time	102.90	1	102.90	2.36	0.15
		C: Temperature	16.27	1	16.27	0.37	0.55
		AB	6.38	1	6.38	0.15	0.71
		AC	12.35	1	12.35	0.28	0.60
		BC	98.27	1	98.27	2.25	0.15
		A <sup>2</sup>	579.39	1	579.39	13.27	<0.0001
		B <sup>2</sup>	1.21	1	1.21	0.03	0.87
		C <sup>2</sup>	49.53	1	49.53	1.13	0.30
LHV	2FI	Model	59.41	6	9.90	36.46	<0.0001
		A: Feed Concentration	0.20	1	0.20	0.72	0.41
		B: Residence Time	0.33	1	0.33	1.22	0.28
		C: Temperature	24.22	1	24.22	89.16	<0.0001
		AB	0.01	1	0.01	0.04	0.84
		AC	6.60	1	6.60	24.29	<0.0001
		BC	0.0007	1	<0.0001	<0.0001	0.96
Gas Yield	2FI	Model	910.61	6	151.77	18.29	<0.0001
		A: Feed Concentration	130.89	1	130.89	15.77	<0.0001
		B: Residence Time	0.0022	1	0.0022	0.0003	0.99
		C: Temperature	439.07	1	439.07	52.91	<0.0001
		AB	22.00	1	22.00	2.65	0.12
		AC	57.48	1	57.48	6.93	0.02
		BC	20.35	1	20.35	2.45	0.13

empirical correlation between the independent variables (inputs/factors) and the measured outcomes (responses), and then RSM was used to statistically analyze the data to obtain the desired results.

The variation in responses such as H2 selectivity, LHV, and total gas yield are evaluated by altering the values of feed concentration, residence time, and reaction temperature. The ANOVA analysis, shown in Table 2, was used to demonstrate the patterns and interactions of the factors/inputs as well as their quadratic effects in analysing the resulting responses/outputs.

This also indicates that the observed characteristics are crucial for evaluating the developed model. The data in Table 2 shows the results of the analysis of variance (ANOVA) for the three observed responses: H2 Selectivity, LHV, and Gas Yield. This analysis helps in understanding the significant effects of independent variables such as Feed Concentration (FC), Residence Time (RT), and Temperature Reaction (TR), as well as the interactions among these variables on the response variables. Although some factors, such as residence time for gas yield and H2 selectivity, exhibit relatively high p-values (> 0.05), these variables were retained in the model to preserve the hierarchical structure of the quadratic model. This retention is consistent with good modeling practice, as excluding such variables may affect the estimation of interaction or quadratic terms that are statistically and practically significant (Brereton, 2019). Moreover, in complex systems like supercritical water gasification, variables with marginal or non-significant p-values can still have meaningful influence due to nonlinear or synergistic interactions, as reflected in the response surface plots and model performance metrics (Li *et al.*, 2023).

3.1.1 H2 Selective

In the H2 Selective response, the model shows an F-value of 16.62 with a p-value of 0.000003, which is highly significant. This indicates that the model is overall effective in explaining the variation in the data. Among all the independent variables, Feed Concentration (A) has the most significant impact with an F-value of 21.38 and a p-value of 0.000331. This suggests that

changes in feed concentration significantly affect H2 selectivity. Conversely, Residence Time (B) and Temperature (C) do not show strong significance with p-values of 0.15 and 0.55, respectively. The interactions between variables (AB, AC, BC) also do not show significant effects. However, the quadratic effect of Feed Concentration (A<sup>2</sup>) is highly significant with a p-value of 0.00, indicating a crucial non-linear relationship between feed concentration and H2 selectivity. The relationship between each variable used to predict the value of H2 Selective can be explained through equation (17).

$$H2\ Selective = -10.039A + 2.60B + 1.13C + 0.0081AB + 0.0050AC - 0.0053BC + 0.16A^2 - 0.00093B^2 - 0.0011C^2 - 172.283$$

(17)

3.1.2 LHV (Lower Heating Value)

In the LHV result, the model shows an F-value of 36.46 with a p-value of < 0.00001, which is also highly significant. This indicates that the model is highly effective in explaining the variation among variables, including at low temperatures. Among the independent variables, Temperature (C) has the most significant impact with an F-value of 89.16 and a p-value of < 0.00001. This suggests that changes in temperature have a very substantial effect on LHV. Feed Concentration (A) and Residence Time (B) do not show significant effects with p-values of 0.41 and 0.28, respectively. However, the interaction between Feed Concentration and Temperature (AC) is significant with a p-value of < 0.00001, indicating that the combination of these two variables significantly affects LHV. The relationship between each variable used to predict the LHV value can be explained through equation (18).

$$LHV = 1.24A + +0.028B + 0.73C - 0.00034AB - 0.0028AC - 0.0053BC$$

(18)

3.1.3 Gas Yield

In the Gas Yield response, the model shows an F-value of 18.29 with a p-value of < 0.00001, indicating a high level of significance. Both Feed Concentration (A) and Temperature (C)

**Table 3**  
DoE Results Based on Face-Centered CCD

	FC	RT	T	LHV Actual (Mj/Nm)	LHV Predict (Mj/Nm)	Total Gas Yield Actual (%)	Total Gas Yield Predict (%)	H2 Selective Actual (%)	H2 Selective Predict (%)
Food Waste	10	20	420	1.38	1.15	8.13	7.72	49.46	46.52
	10	20	460	2.58	2.93	11.37	11.87	46.75	48.97
	10	20	500	4.95	4.7	17.67	16.02	46.21	47.72
	10	40	420	1.68	1.54	8.93	8.47	50.09	54.32
	10	40	460	2.79	3.31	12.97	14.51	53.68	52.51
	10	40	500	5.19	5.08	18.53	20.55	51.65	47
	10	60	420	2.21	1.93	10.58	9.23	58.85	61.37
	10	60	460	3.26	3.69	14.77	17.16	63.98	55.3
	10	60	500	6.25	5.45	20.85	25.09	51.89	45.53
	2	60	500	6.83	6.92	28.27	24.81	89.33	85.74
	6	60	500	6.52	6.18	22.69	24.95	57.25	62.96
	10	60	500	6.25	5.45	20.85	25.09	51.89	45.53
Agricultural Waste	20	40	500	3.47	3.3	25.4	23.65	25.4	25.13
	20	40	350	1.15	0.9078	13.4	13.52	20.3	19.14
	20	40	400	1.16	1.7	16.2	16.89	25.9	26.92
	20	40	450	2.86	2.5	22	20.27	27.5	28.92
	20	40	500	3.47	3.3	25.4	23.65	27.9	25.13
	20	20	500	2.54	2.98	18.2	21.86	23.1	24.21
	20	40	500	3.52	3.3	25.7	23.65	27.5	25.13
	20	60	500	3.56	3.61	27.3	25.44	27.1	25.28
	20	80	500	3.66	3.92	26.4	27.23	26.6	24.69
	10	60	500	4.27	5.45	29.7	25.09	27.4	45.53
	15	60	500	3.96	4.53	28.4	25.26	27.2	31.23
	20	60	500	3.56	3.61	27.3	25.44	27.1	25.28
	25	60	500	3.02	2.68	22	25.61	23.7	27.67

have significant effects on gas yield, with F-values of 15.77 and 52.91, respectively, and p-values of < 0.00001. This suggests that changes in feed concentration and temperature significantly impact the amount of gas produced. Residence Time (B) does not show significance with a p-value of 0.99. The interactions between Feed Concentration and Temperature (AC) and between Residence Time and Temperature (BC) show significant effects with p-values of 0.02, indicating that these interactions are also important in determining gas yield. However, the quadratic effects of each variable do not show high significance. The relationship between each variable used to predict the Gas Yield value can be explained through equation (19).

Gas yield = 1,24A + 0,028B +  
0.073C - 0.00034AB - 0.0028AC - 0.0053BC

(19)

From the equations explained previously, predictive data for each factor value were obtained. The actual and predicted data from the developed Central Composite Design (CCD) model are shown in Table 3.

The proposed model was then evaluated to obtain normalized and appropriate data using normal plots for residuals and outliers. In this study, it is expected that the model does not follow any trends or order and that the data points

should be close to a straight line. Figure 2 shows the residual and outlier plot for H2 Selective.

Figure 2a illustrates the trend of data from the H2 Selective response, where the random distribution of data points indicates normal distribution and confirms the model's predictability. This figure also includes an outlier plot for H2 Selective production, with upper and lower outlier limits of ±3.78739, where data points outside these limits are considered outliers. Figure 2b displays the LHV data points, all within the range of ±3.64577, and its normal plot in Figure 2b further demonstrates normal distribution of the experimental data. Additionally, Figure 2c presents the normal plot of residuals and outliers for gas yield production, where all data points are normally distributed, close to the reference line, and fall within the outlier bounds of ±3.64577, confirming data consistency and normal distribution.

The development of the DoE model using the RSM method requires validation and verification processes as the final stages of model development. The previously obtained equations (17-19) are then compared with experimental data. The comparison graph between predicted and experimental data is shown in Figure 3. This figure presents the validation of the RSM model in predicting H2 selectivity, Gas Yield, and LHV from supercritical water gasification. The close alignment of the predicted values with experimental data across all runs confirms the robustness and reliability of the RSM model. Such graphical



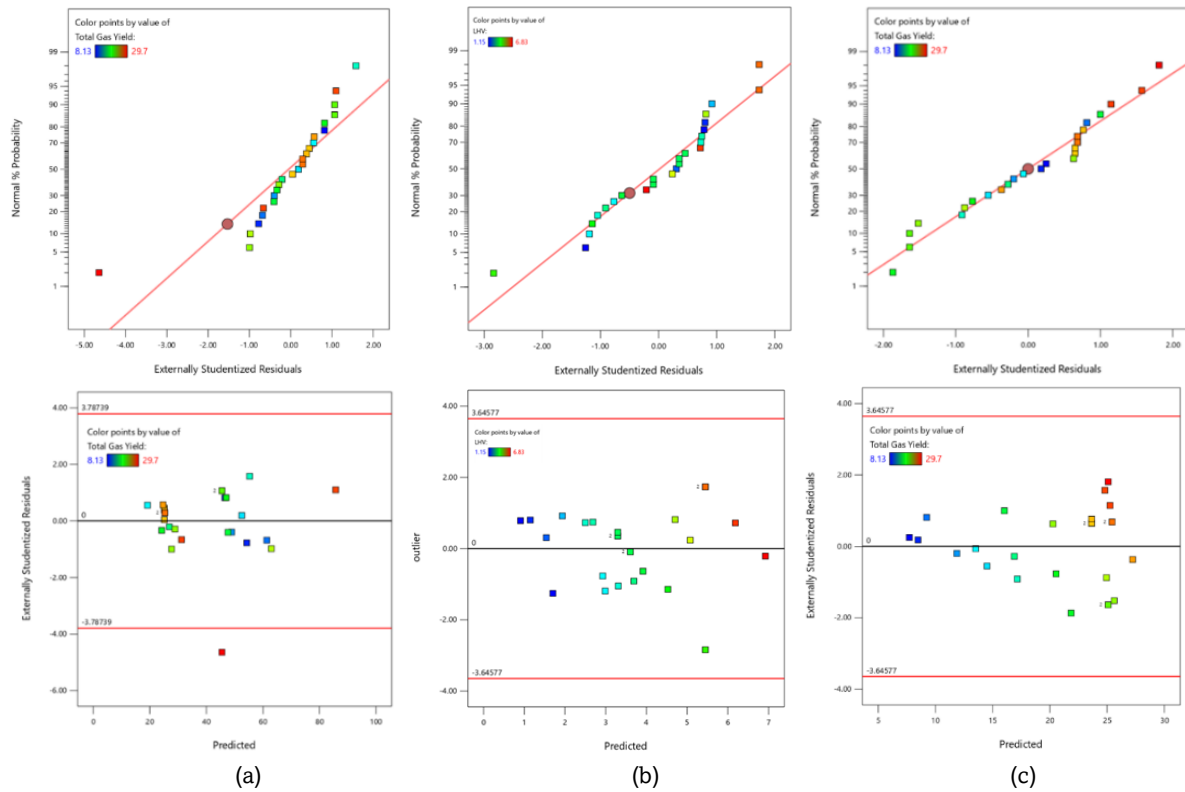


**Fig. 2** The Normal Plot of Residuals and Outliers for (a) H<sub>2</sub> Selective, (b) LHV, and (c) Gas Yield

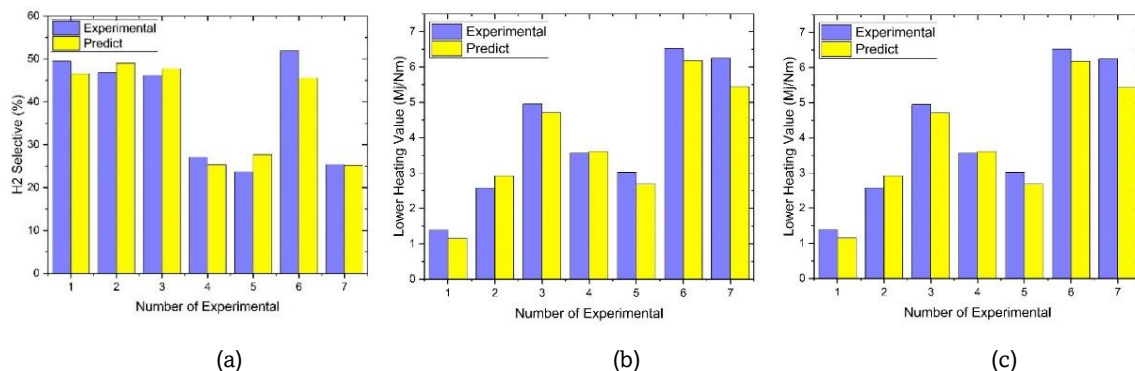


**Fig. 3** Model Validation of RSM for (a) H<sub>2</sub> Selectivity, (b) LHV, and (c) Gas Yield

representation complements the numerical results presented in Table 3, reinforcing the model's capability in simulating SCWG performance effectively.

In the following surface plots (Figures 4–6), trends are visually represented using color gradients. Darker or red-colored zones indicate higher values of the response variable, while lighter or blue zones indicate lower values. These gradients effectively serve as implicit trendlines, highlighting optimal regions and the influence of each parameter. Figure 4 illustrates various parameters affecting H<sub>2</sub> Selectivity through 2D and 3D curves, highlighting the impact of different variables. Figures 4a-c show that increasing the feed concentration from 2% to around 15.8% significantly boosts H<sub>2</sub> selectivity, reaching a peak at the highest concentration. Residence time also plays a crucial role, with a notable increase in H<sub>2</sub> selectivity observed when the residence time is extended from 20 to 70 minutes, especially at high feed concentrations. Different feed concentrations and residence times suggest that higher temperatures and longer residence times generally enhance gasification efficiency and H<sub>2</sub> selectivity (Ibtissem *et al.*, 2019;

Yang *et al.*, 2022). However, at very high feed concentrations (around 20.4%), H<sub>2</sub> selectivity decreases if the residence time is insufficiently long. At lower temperatures (around 350-400°C) and longer residence times (70-80 minutes), H<sub>2</sub> selectivity remains high, whereas at very high temperatures (around 500°C) or short residence times (20-30 minutes), H<sub>2</sub> selectivity drops significantly. Higher temperatures and longer residence times improve gasification efficiency and support H<sub>2</sub> production (Chen *et al.*, 2022; Li *et al.*, 2023). Figure 4c further explains that at lower temperatures (350-400°C) and shorter residence times (20-40 minutes), H<sub>2</sub> selectivity tends to be low. When the temperature increases to 440-500°C and the residence time extends to around 70 minutes, H<sub>2</sub> selectivity moderately increases due to enhanced biomass conversion and hydrogen production. During the reaction, the hydrogen gas fraction increases while the CO and CO<sub>2</sub> gas fractions decrease, indicating that longer residence times allow the water-gas shift reaction to reach equilibrium, thus improving hydrogen production and gasification efficiency (Cao *et al.*, 2022).



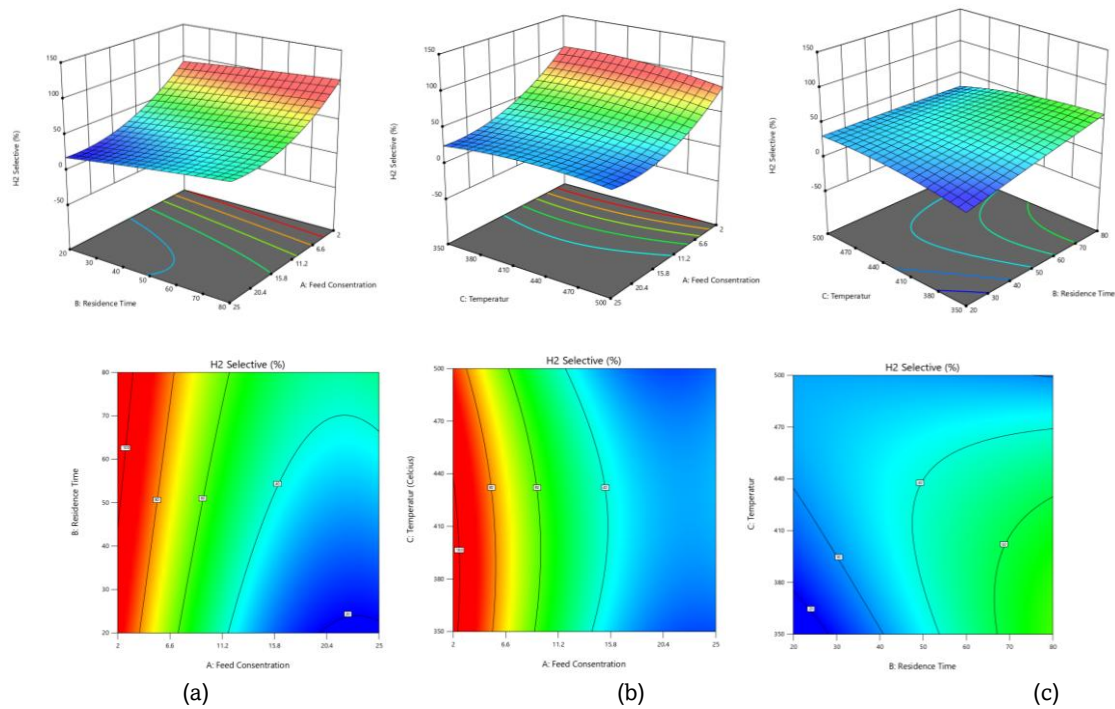


**Fig. 4** 2D and 3D Contour Plots for H<sub>2</sub> Selective Production Based on the Impact of (a) Residence Time and Feed Concentration, (b) Temperature and Feed Concentration, (c) Residence Time and Temperature

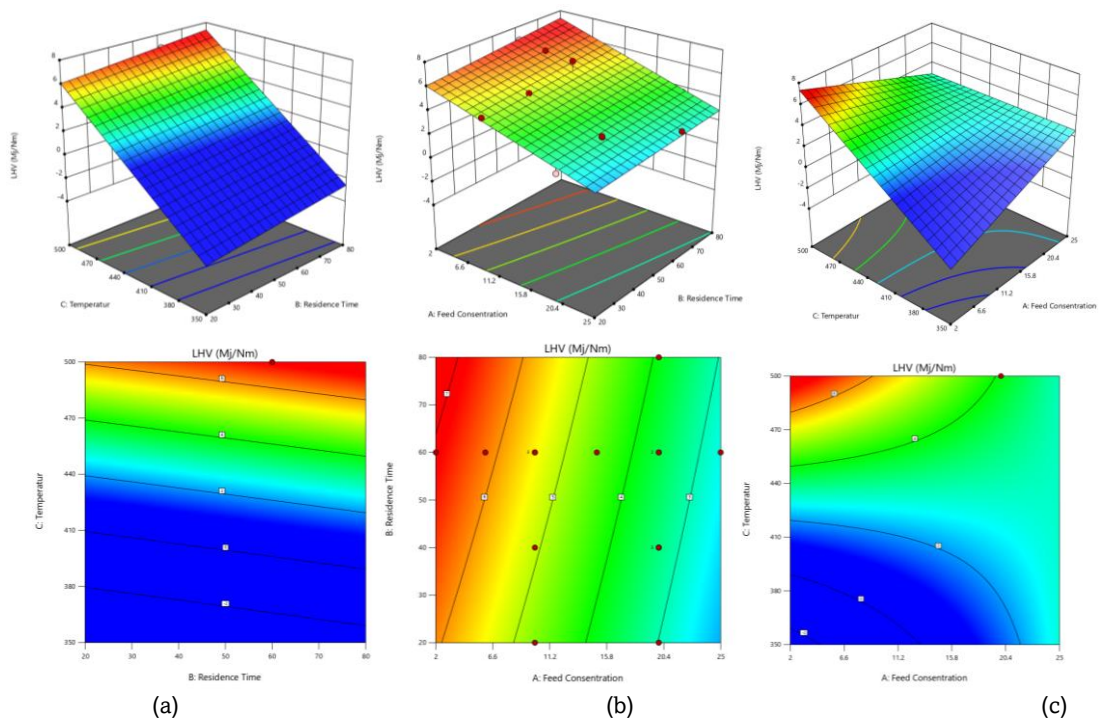


**Fig. 5** 2D and 3D Contour Plots for LHV Concentration Based on the Impact of (a) Residence Time and Temperature, (b) Residence Time and Feed Concentration, (c) Feed Concentration and Temperature

Figure 5a illustrates the relationship between temperature and residence time on the LHV. At lower temperatures (approximately 350 to 410°C) and shorter residence times (around 20 to 40 minutes), the LHV tends to be lower. However, when the temperature is increased to the range of 410 to 500°C and the residence time is extended to approximately 70 to 80 minutes, a significant increase in LHV is observed. This relationship is indirectly supported by findings related to gasification efficiency, suggesting that higher temperatures and

longer residence times not only enhance gasification efficiency but also positively impact the LHV of the produced gas (Li *et al.*, 2018; Li *et al.*, 2023). Figure 5b further elucidates that optimal LHV is achieved when both feed concentration and residence time are maintained at high values. Specifically, a feed concentration of approximately 20.4% and a residence time between 60 to 80 minutes result in gas with high LHV content. It is noteworthy that while high feed concentrations can reduce exergetic efficiency, thereby affecting LHV values, an

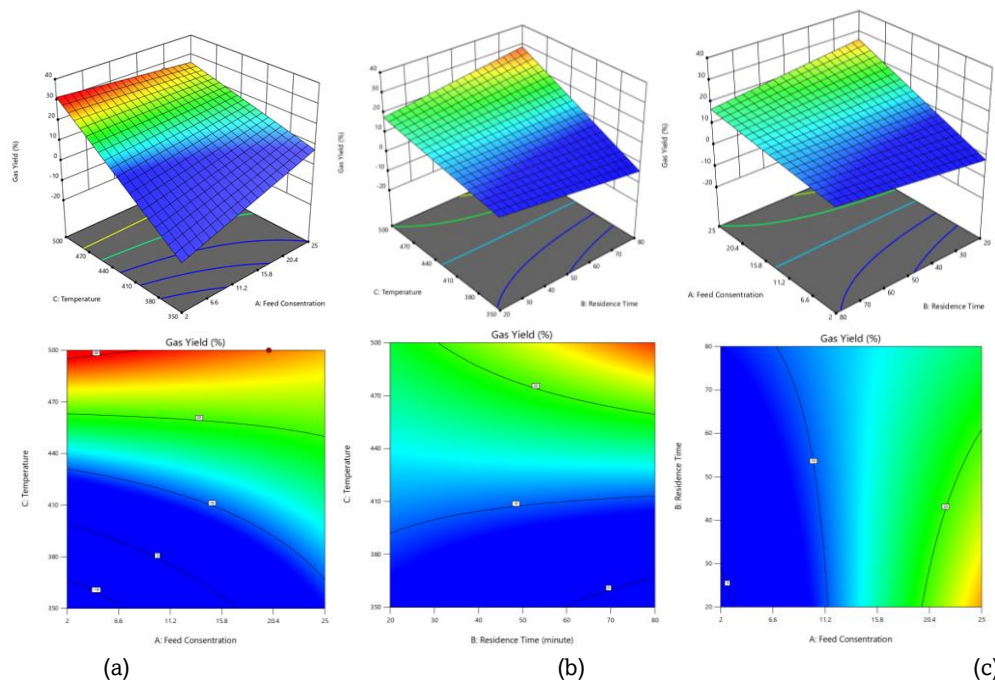


**Fig. 3** 2D and 3D Contour Plots for Gas Yield Production Based on the Impact of (a) Residence Time and Temperature, (b) Residence Time and Feed Concentration, (c) Feed Concentration and Temperature

appropriate combination of factors, such as residence time, is essential to achieve high LHV values (Zhang *et al.*, 2019).

Figure 5c the data demonstrates that increasing both temperature and feed concentration generally leads to an increase in LHV. At lower temperatures (around 350°C) and low feed concentrations (around 2%), the LHV is correspondingly low. However, as the temperature rises to approximately 500°C and the feed concentration increases to around 25%, the LHV increases significantly. The optimal combination for achieving the highest LHV is identified at a temperature of approximately 500°C and a feed concentration of around 25%, where the LHV reaches its peak value of approximately 6 to 8 MJ/Nm<sup>3</sup>. The interaction between feed concentration and temperature plays a critical role in determining the efficiency of the gasification process and the resulting LHV, with higher temperatures generally enhancing exergetic efficiency (Zhang *et al.*, 2019).

Additionally, Figure 5 provides insights into various parameters affecting gas yield production, as depicted through 2D and 3D curves. According to Figure 5a, at lower temperatures (around 350°C) and low feed concentrations (around 2%), gas yield production is low. Conversely, as the temperature increases to approximately 500°C and the feed concentration rises to around 25%, the total gas yield shows a significant increase. This indicates that both temperature and feed concentration have a substantial impact on gas yield production. Empirical studies have consistently demonstrated that higher temperatures can produce relatively high gas yields, and feed concentrations in the range of 15-20% also contribute to increased gas yield (Qiu *et al.*, 2024; C. Yang *et al.*, 2021).

Figure 6a demonstrates that both temperature and residence time significantly impact total gas yield. At lower temperatures (around 350°C) and shorter residence times (around 20 minutes), the gas yield is low. However, as the temperature rises to approximately 500°C and the residence time extends to around 80 minutes, the total gas yield increases substantially. This suggests that a combination of higher temperature and longer residence time results in a higher total gas yield, as increased temperature promotes the reaction rate

and the formation of hydrogen and methane, enhancing gasification efficiency and gas yield production (Zhao *et al.*, 2020; Li *et al.*, 2023). Nevertheless, it is important to note that at certain temperatures and residence times, the gas yield may decline. Initially, increasing residence time can enhance gas yield, but excessively long residence times can decrease exergetic efficiency and gas production (Zhang *et al.*, 2019).

Figure 6c illustrates that increasing feed concentration and residence time significantly impacts total gas yield. At lower feed concentrations (around 2%) and shorter residence times (around 20 minutes), the gas yield is low. However, as the feed concentration increases to around 25% and the residence time extends to around 80 minutes, gas yield production significantly increases.

The research findings reveal significant challenges in optimizing influential parameter values for supercritical water gasification (SCWG) to produce H<sub>2</sub> selectivity, LHV, and gas yield, which are characteristics of syngas from the gasification process. To achieve optimal syngas characteristics, each variable requires careful optimization. Thus, Response Surface Methodology was used to ensure high H<sub>2</sub> selectivity production within specific residence times and temperatures, as illustrated in Figure 7. The ramp function of the optimal solution achieves impressive results, with H<sub>2</sub> selectivity, LHV, and gas yield values of 84.73%, 6.95 MJ/Nm<sup>3</sup>, and 29.7%, respectively. This figure visually demonstrates the contribution of each input variable: feed concentration, residence time, and temperature, toward the desired responses. It can be observed that both residence time and temperature exhibit steep response slopes, indicating their dominant influence in enhancing syngas characteristics, particularly H<sub>2</sub> selectivity. In contrast, feed concentration has a relatively limited effect, as reflected in its gentler gradient across all response profiles. These findings confirm that temperature and residence time are the most critical factors in maximizing the SCWG performance, while feed concentration only plays a minor role unless combined

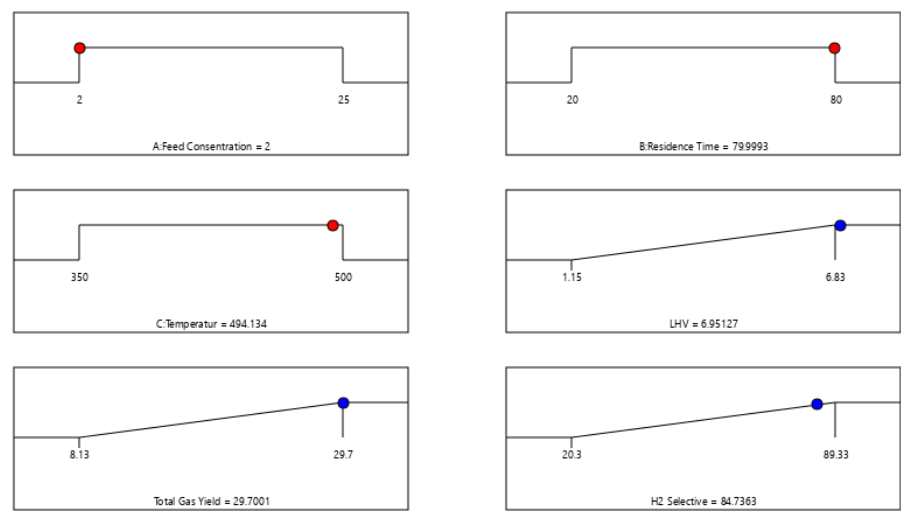


Fig. 4 Ramp function of RSM Optimization

with elevated temperature and sufficient reaction time. The trends observed in the ramp function are also consistent with the surface plots presented in Figures 4-6, reinforcing the reliability of the optimization outcome.

Therefore, careful attention must be given to optimizing the combination of process variables to achieve maximum efficiency as they directly affect the syngas characteristics produced. Based on the RSM optimization results, to reach the

optimal result, a feed concentration of 2%, combined with temperature and residence time of 490-495°C and 80 minutes, respectively, is required. This study emphasizes the importance of meeting the input variables obtained from the optimization results to produce syngas characteristics rich in hydrogen. However, accurately determining SCWG process parameters becomes highly complex and requires validation through various methods. Additionally, factors such as biomass content,

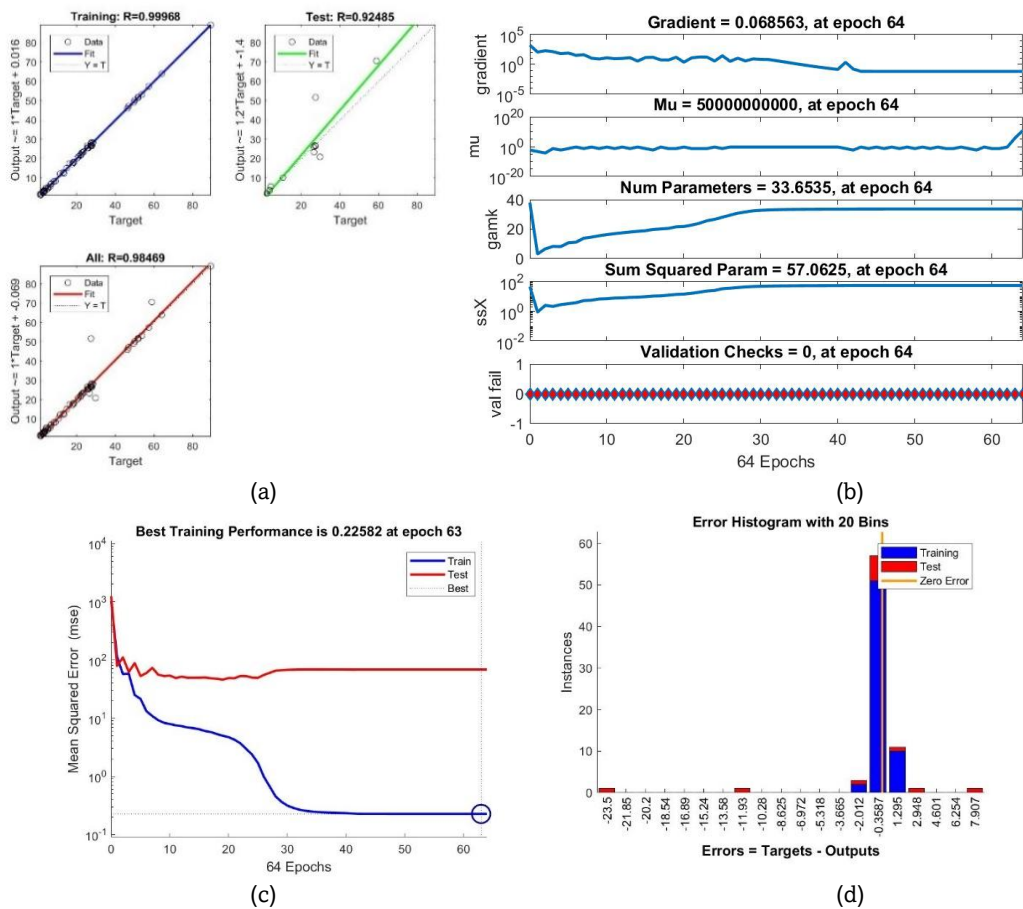


Fig. 8 (a) ANN Regression Data, (b) Training State, (c) Validation Performance, (d) Error Histogram



pressure, and catalysts must be considered to develop the most effective SCWG process for producing hydrogen-rich syngas with a high LHV.

### 3.2 ANN Modelling

Artificial Neural Network (ANN) modelling is employed to determine the relationship between input and output variables. This analysis is conducted through several stages, including data collection, network development and configuration, initialization of weights and biases, training, and testing. The optimal selection of neurons is based on the maximum regression parameter (R) with the minimum Mean Square Error (MSE). This strategy is in line with the approach taken by Popoola *et al.* (2019), who stated that variations in the number of hidden neurons and the selection of training algorithms significantly affected the performance of the ANN model, where the best configuration gave an R-value of 0.99 and an RMSE of 0.81 (Popoola *et al.*, 2019). Similar optimization approaches were also observed in studies by (DEMİRBAY & KARAKULLUKÇU, 2020), where the use of 8 neurons in the hidden layer with a Bayesian-optimized backpropagation algorithm resulted in the lowest MSE and highest regression accuracy.

In this study, the ANN model consists of three inputs, one hidden layer with five neurons, and three target outputs. A trial-and-error method is used to achieve the optimal design, selecting the architecture with the lowest error (RMSE) and the best regression coefficient. The performance of each architecture is further evaluated using Mean Absolute Error (MAE) and Root Mean Square Error (RMSE), as defined in Equations (13) and (14), which quantify the average and squared deviations between predicted and actual values, respectively. This method of performance evaluation is widely adopted in various ANN applications, including environmental modeling and energy system forecasting, where MAE and RMSE are

considered reliable indicators of prediction accuracy (Córdoba *et al.*, 2023; Farooq *et al.*, 2022).

Figure 1 illustrates the architecture of the observed artificial neural network. The difference between the model output and the desired data is known as the network error rate. The backpropagation algorithm enables neurons to learn new information during the testing phase by adjusting weights to reach the optimal point, significantly reducing the error value. The effectiveness of backpropagation in refining model accuracy has been validated in multiple studies, showing its ability to improve learning in both small and large datasets (Kavitha Mayilvaganan & Naidu, 2011).

The results indicate that a regression coefficient value close to 1 result in a more accurate trendline. Figure 8a presents several regression coefficient models and comparisons between the regression and ANN models during training, testing, and overall results. In the training phase (Training:  $R=0.99968$ ), a regression coefficient (R) value of 0.99968 suggests an almost perfect correlation between the model's predicted results and the target values, indicating excellent model performance. During testing (Test:  $R=0.92485$ ), a regression coefficient (R) value of 0.92485 still indicates a strong correlation, though slightly lower than during training. The combined data (All:  $R=0.98469$ ) shows a regression coefficient (R) value of 0.98469, demonstrating that the ANN model has very good and accurate predictive capability overall. This level of accuracy is consistent with the performance reported in similar ANN-based predictive models in energy, environmental, and materials science domains (Córdoba *et al.*, 2023; Farooq *et al.*, 2022).

Figures 8b-d display the training state, ANN model performance, and error histogram results. The training state indicates that when the MSE of the validation sample increases, training automatically stops. Variations in the gradient coefficient are also observed due to the number of epochs. The error histogram shows the difference between target and prediction values after training, explaining various patterns of

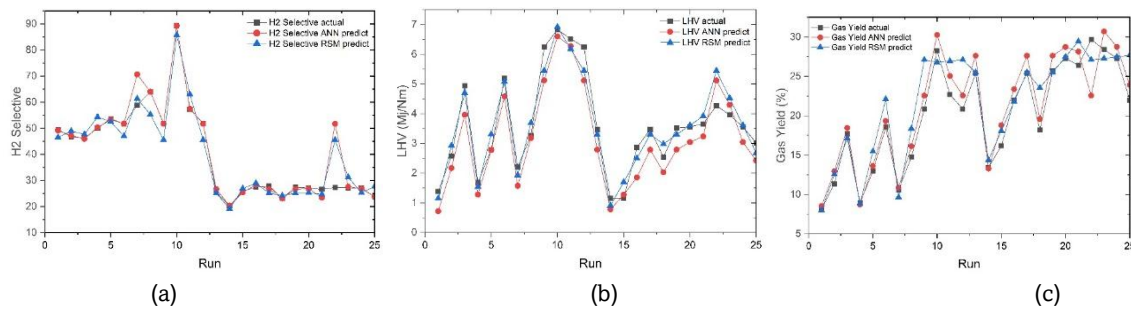


**Fig. 9** Actual Values versus Correlation Values of ANN and RSM for (a) H2 Selective, (b) LHV, (c) Gas Yield

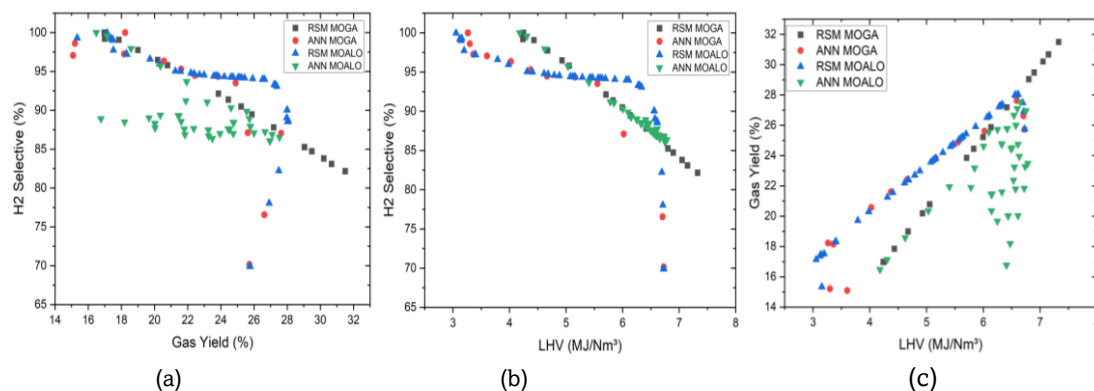


**Fig. 5** Comparison of MOGA RSM, MOGA ANN, MOALO RSM, and MOALO ANN for (a) H2 Selective vs Gas Yield, (b) H2 Selective vs LHV, (c) Gas Yield vs LHV

expected levels and goals, with the performance graph illustrating the network's best validation efficiency. To predict the target data for H<sub>2</sub> selectivity, LHV, and gas yield, the experimental equation model obtained based on Figure 8a is output = 1 \* target + 0.069, with the performance plot in Figure 8c, showing the training process stopping at 0.22582 at epoch 63 within the allowed data range.

Figure 9 illustrates the relationship graph of actual data with RSM and ANN values. Figures 9a-c show that both ANN and RSM can predict LHV values with good accuracy, with ANN demonstrating an advantage in terms of prediction accuracy and consistency. This advantage is likely due to the regression coefficient result with an R-value of 0.98. This high R<sup>2</sup> value indicates that the ANN model can capture and replicate the fundamental relationships in the data with high fidelity, making its predictive values more accurate. This finding aligns with results from recent studies on gasification modeling. Umar *et al.* (2024) applied an ANN model with a 3–10–2 architecture for co-gasification of oil palm biomass and reported that it significantly outperformed RSM, achieving R<sup>2</sup> values above 0.95 and maintaining robustness across varying operating conditions (Umar *et al.*, 2024). Similarly, Ramaswamy *et al.* (2023) demonstrated that ANN provided more accurate predictions of syngas composition particularly for H<sub>2</sub> and CO during the gasification of Aegle Marmelos shell. Their analysis showed that ANN was better suited to capturing the influence of parameters such as moisture content and particle size due to its capability to represent nonlinear process dynamics (Ramaswamy *et al.*, 2025). These findings emphasize that ANN offers more reliable and generalizable performance than RSM when applied to thermochemical systems like gasification, where multiple input parameters interact in complex, nonlinear ways.

### 3.3 MOGA and MOALO Optimization

The analysis of the Multi-Objective Genetic Algorithm (MOGA) and Multi-Objective Ant Lion Optimization (MOALO) was conducted using MATLAB software to generate Pareto charts for three objective functions: H<sub>2</sub> selectivity, LHV, and gas yield. The optimization process also utilized estimations derived from the Design of Experiments (DoE) in equations (17)–(19). These three objective values were then maximized to obtain hydrogen-rich syngas with a high LHV. Furthermore, the MOGA and MOALO analyses were performed based on estimations from an Artificial Neural Network (ANN). The input ranges for feed concentration, residence time, and reaction temperature were determined based on previous experimental data. The constructed network function demonstrated high accuracy in predicting H<sub>2</sub> selectivity, LHV, and gas yield values. The function derived from the ANN was subsequently used as the fitness function in the optimization process.

This approach is consistent with recent developments in syngas optimization using artificial intelligence. Rawat *et al.* (2024) demonstrated that integrating ANN with MOGA in a co-pyrolysis system resulted in significantly higher hydrogen (54.5%) and methane yields compared to RSM-based optimization, emphasizing the superior capability of ANN-MOGA in handling complex nonlinear interactions (Rawat *et al.*, 2024). Similarly, Ramaswamy *et al.* (2023) reported that ANN outperformed RSM in predicting syngas composition during biomass gasification, particularly in capturing the effects of moisture content and particle size (Ramaswamy *et al.*, 2025). In another study, Abioye *et al.* (2024) compared the performance of ANN and RSM in co-gasifying palm oil decanter cake and alum sludge, concluding that ANN produced more reliable

predictions with a coefficient of determination (R<sup>2</sup>) of 0.971 (Abioye *et al.*, 2024).

Comparison of MOGA RSM, MOGA ANN, MOALO RSM, and MOALO ANN for each output variable, including (a) H<sub>2</sub> Selectivity vs. Gas Yield, (b) H<sub>2</sub> Selectivity vs. LHV, and (c) Gas Yield vs. LHV, is presented in Figure 10. This figure illustrates the distribution of optimal solutions obtained from each method, where the plotted points represent the range of predicted values from the entire population of Pareto-optimal solutions or only the final selected outputs. The optimization values generated through the Design of Experiments (DoE) equations are represented by MOGA RSM and MOALO RSM values. The Pareto chart reveals that the highest values achieved for H<sub>2</sub> selectivity, LHV, and gas yield are 100%, 31.50%, and 7.33 MJ/Nm<sup>3</sup> for MOGA RSM, respectively, and 100%, 27.53%, and 6.78 MJ/Nm<sup>3</sup> for MOALO RSM, respectively. The minimum values obtained from the optimization are 82.16%, 16.97%, and 4.24 MJ/Nm<sup>3</sup> for MOGA RSM, and 86.05%, 16.48%, and 4.17 MJ/Nm<sup>3</sup> for MOALO RSM, indicating that the optimization results via DoE equations fall within the same range. These results indicate that MOGA RSM outperforms MOALO RSM in maximizing gas yield and LHV, while MOALO RSM provides better H selectivity.

Figure 10 also depicts the optimization values generated through the Artificial Neural Network (ANN) model using the Bayesian Regularization method, as indicated by the Pareto chart. Optimization using the MOGA ANN prediction model yielded maximum ideal values for H<sub>2</sub> selectivity, LHV, and gas yield of 100%, 27.63%, and 6.73 MJ/Nm<sup>3</sup>, respectively, with the lowest optimization values being 70.17%, 15.09%, and 3.26 MJ/Nm<sup>3</sup>, respectively. Similarly, the maximum ideal value MOALO ANN prediction model for H<sub>2</sub> selectivity, LHV, and gas yield are 99.98%, 28.05%, and 6.72 MJ/Nm<sup>3</sup>, respectively, with the lowest optimization values being 69.89%, 15.33%, and 3.05 MJ/Nm<sup>3</sup>, respectively.

These results demonstrate that the MOALO and MOGA ANN prediction models have relatively similar value ranges. Overall, the distribution patterns in the Pareto charts reveal that ANN-based methods are more capable of reaching ultra-high H<sub>2</sub> selectivity, while DoE-based methods, especially MOGA RSM, show a strength in optimizing gas yield and energy value (LHV), offering distinct advantages depending on the syngas performance target.

The optimization values obtained using the TOPSIS method for MOGA and MOALO, generated through MATLAB software, and the optimization values for Response Surface Methodology (RSM) through Design Expert software, can be utilized to

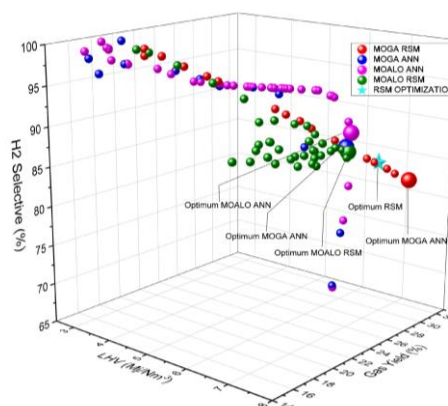


**Fig. 6** 3D plot MOGA RSM, MOGA ANN, MOALO ANN, MOALO RSM, and RSM Optimization

**Table 4**  
Comparison of the optimal value results from each model

Optimization Method	Feed Conosentration (wt%)	Residence Time (s)	Temperature Reaction (C)	H2 Selective (%)	Gas yield (%)	LHV (Mj/Nm)
MOGA RSM	2	80	500	82.16	31.5	7.33
MOGA ANN	2.27	58.63	499.89	87.03	27.63	6.59
MOALO RSM	2	76.28	491.06	86.52	27.54	6.65
MOALO ANN	2.01	50.22	500	88.69	28.05	6.61
RSM Optimization	2	80	494.13	84.736	29.07	6.951

determine the optimal values for each optimization method. As depicted in Figure 11, which presents a 3D plot comparative analysis of various optimization methods such as MOGA RSM, MOALO RSM, MOGA ANN, MOALO ANN, and RSM optimization for the Supercritical Water Gasification (SCWG) process. The red spheres in the Pareto chart represent the optimization values of the MOGA RSM model, where the optimal point for this model is at an H2 selectivity of 82.16%, a Gas Yield of 31.50%, and an LHV of 7.33 MJ/Nm<sup>3</sup>. This indicates that the MOGA RSM method is highly effective in achieving high gas yields at high LHV values, with reasonably good H2 selectivity. The selection of this optimal point is suitable for applications prioritizing high gas production with adequate hydrogen efficiency. The MOGA ANN model, represented by blue spheres in the Pareto chart, shows the optimal point of this optimization model at an H2 selectivity of 87.03%, a Gas Yield of 27.63%, and an LHV of 6.59 MJ/Nm<sup>3</sup>, indicating greater variability in H2 selectivity with similar LHV and gas yield values compared to MOGA RSM.

The optimization values with the MOALO RSM model are represented by green spheres in Figure 11, where the ideal optimization point for this model is at an H<sub>2</sub> selectivity of 86.52%, a Gas Yield of 27.54%, and an LHV of 6.65 MJ/Nm<sup>3</sup>. For the MOALO ANN model, the ideal optimization point obtained is at an H<sub>2</sub> selectivity of 88.69%, a Gas Yield of 28.06%, and an LHV of 6.61 MJ/Nm<sup>3</sup>. Overall, MOALO ANN is superior in maximizing the total gas yield and shows higher potential H<sub>2</sub> selectivity at some optimal points compared to MOALO RSM. However, MOALO RSM demonstrates more consistent H<sub>2</sub> selectivity.

The RSM optimization method is represented by green stars, marking the optimal point achieved through RSM Optimization, indicating an H<sub>2</sub> selectivity of 84.736%, a Gas Yield of 29.07%, and an LHV of 6.951 MJ/Nm<sup>3</sup>. This balance of results makes it optimal for applications requiring good overall performance. The selection of the optimization model depends on the application's priorities, whether it prioritizes high total gas yield or higher H<sub>2</sub> selectivity. MOGA RSM excels in total gas yield, while MOALO ANN excels in H<sub>2</sub> selectivity. RSM optimization shows a good balance between the two.

Table 4 presents the results of each optimization method, focusing on factors such as feed concentration, residence time, and reaction temperature, as well as response variables including H<sub>2</sub> selectivity, gas yield, and LHV. The parameter values fall within the ranges shown in Table 3, which includes actual data. Overall, based on the table, MOGA RSM excels in total gas yield, while MOALO ANN is superior in H<sub>2</sub> selectivity. RSM optimization demonstrates a good balance between the two. By analyzing these optimal values, it is evident that each method offers distinct advantages depending on the specific goals of the application. For high total gas yield, MOGA RSM is the preferred choice. For high H<sub>2</sub> selectivity, MOALO ANN is

the most effective. For a balanced performance, RSM optimization is the optimal method.

Although optimization results identified a feed concentration of 2 wt% as optimal for maximizing H<sub>2</sub> selectivity, its application at the industrial scale poses practical challenges. The process requires handling highly diluted biomass at such low concentrations, leading to increased water usage, larger reactor volumes, and higher energy demand for pressurization and heating to supercritical conditions. These factors may significantly raise operational costs and affect the system's economic viability. Thus, while the 2 wt% condition is useful for determining theoretical performance limits, moderately higher concentrations (e.g., 5–15 wt%) may offer a more realistic balance between energy input and hydrogen yield in practical applications.

Regarding the optimization methods, the choice between MOGA and MOALO should align with the objectives of the optimization task. MOGA demonstrated faster convergence and broader solution diversity, making it suitable for early-stage design and sensitivity analysis. In contrast, MOALO showed better performance in avoiding local optima and achieved slightly higher H<sub>2</sub> selectivity, suggesting its advantage in later-stage process refinement where precision is critical.

Future research should integrate these optimization findings with techno-economic assessments and process simulation to ensure industrial relevance. Aspen Plus or SuperPro Designer can support detailed evaluations of energy use, heat integration, and utility requirements. Additionally, incorporating life-cycle assessment (LCA) and cost-benefit analysis would offer valuable insights into environmental and economic trade-offs, facilitating the transition of SCWG from conceptual research to commercially feasible solutions.

4. Conclusion

This study integrates Response Surface Methodology (RSM), Artificial Neural Networks (ANN), and Multi-Objective Genetic Algorithm Optimization (MOGA) to optimize the Supercritical Water Gasification (SCWG) process for producing hydrogen-rich syngas from solid waste. The results demonstrate that the MOGA RSM approach achieves optimal values with an H<sub>2</sub> selectivity of 82.16%, a gas yield of 31.50%, and an LHV of 7.33 MJ/Nm<sup>3</sup>, making it highly effective for applications requiring high gas yields at high LHV values. Conversely, the MOGA ANN model shows optimal values with an H<sub>2</sub> selectivity of 87.03%, a gas yield of 27.63%, and an LHV of 6.59 MJ/Nm<sup>3</sup>, indicating greater variability in H<sub>2</sub> selectivity with similar LHV and gas yield values compared to MOGA RSM. MOALO RSM achieves ideal optimization values with an H<sub>2</sub> selectivity of 86.52%, a gas yield of 27.54%, and an LHV of 6.66 MJ/Nm<sup>3</sup>, demonstrating good consistency in H<sub>2</sub> selectivity. Meanwhile, the MOALO ANN model excels in maximizing gas yield with



optimal values of H<sub>2</sub> selectivity at 88.69%, a gas yield of 28.06%, and an LHV of 6.61 MJ/Nm<sup>3</sup>, showing higher potential H<sub>2</sub> selectivity at some optimal points compared to MOALO RSM. The RSM optimization method provides a balanced performance with optimal values of H<sub>2</sub> selectivity at 84.736%, a gas yield of 29.07%, and an LHV of 6.951 MJ/Nm<sup>3</sup>, making it suitable for applications requiring good overall performance.

Key factors influencing hydrogen production include reaction temperature and residence time, where higher temperatures and longer residence times generally enhance hydrogen yield. Feed concentration must be carefully balanced to optimize syngas output and energy efficiency, as higher concentrations can reduce hydrogen yield. ANN models provided highly accurate predictions with R<sup>2</sup> values exceeding 0.95, validating their effectiveness for predictive analysis in the SCWG process. Both MOGA and MOALO algorithms effectively identified optimal process parameters, illustrated through Pareto charts, highlighting trade-offs between H<sub>2</sub> selectivity, gas yield, and LHV. The TOPSIS method was employed to rank the optimal solutions generated by MOGA and MOALO, providing a clear methodology to select the best alternative based on proximity to the ideal solution.

The combined use of RSM, ANN, and MOGA/MOALO offers a robust framework for optimizing SCWG processes. While the predictive models demonstrated strong performance with R<sup>2</sup> values exceeding 0.95, further validation using independent datasets or pilot-scale experimentation is recommended to improve the robustness and applicability of the proposed models. The integration of response surface plots, regression models, and Pareto-based optimization contributes to improved interpretability by illustrating parameter interactions and trade-offs across multiple objectives. The optimized conditions, particularly those achieving high hydrogen selectivity and elevated LHV, provide a practical reference for industrial SCWG system development. Future studies should incorporate techno-economic analysis and environmental impact assessments to evaluate the broader feasibility and sustainability of this approach.

## Acknowledgments

The authors would like to express their profound gratitude to Prof. Dr.-Ing. Nasruddin and other lecturers of the Design of Experiment course, as well as to fellow master's students specializing in energy conversion at the University of Indonesia, for their invaluable support and guidance throughout this research. We also extend our sincere thanks to the Indonesia Endowment Fund for Education (LPDP) of the Ministry of Finance for their funding, which made this research possible.

**Author Contributions:** B.A.S.: Conceptualization, methodology, formal analysis, writing—original draft, A.S.; supervision, resources, project administration, W.R.S.; writing—review and editing, project administration, validation, H.D.; supervision, project administration, validation. P.L.: writing original draft, Investigation, I.A.Q.: data curation, visualization. All authors have read and agreed to the published version of the manuscript. All authors have read and agreed to the published version of the manuscript.

**Funding:** This research was funded by The Indonesia Endowment Funds for Education (LPDP) Ministry of Finance.

**Conflicts of Interest:** The authors declare no conflict of interest.

## References

- Abioye, K. J., Harun, N. Y., Arshad, U., Sufian, S., Yusuf, M., Jagaba, A. H., Ighalo, J. O., Al-Kahtani, A. A., Kamyab, H., Kumar, A., Prakash, C., Okolie, J. A., & Ibrahim, H. (2024). Response surface methodology and artificial neural network modelling of palm oil decanter cake and alum sludge co-gasification for syngas (CO+H<sub>2</sub>) production. *International Journal of Hydrogen Energy*, 49, 200–214. <https://doi.org/10.1016/j.ijhydene.2024.06.397>
- Aentung, T., Wu, W., & Patcharavorachot, Y. (2024). Process design and multi-objective optimization of solid waste/biomass co-gasification considering tar formation. *Journal of the Taiwan Institute of Chemical Engineers*, 164. <https://doi.org/10.1016/j.jtice.2024.105688>
- Albarelli, J. Q., Mian, A., Santos, D. T., Ensinas, A. V., Maréchal, F., & Meireles, M. A. A. (2017). Multi-objective optimization of supercritical water gasification of leftover Brazilian ginseng roots after phytochemical recovery steps. *Brazilian Journal of Chemical Engineering*, 34(3), 841–850. <https://doi.org/10.1590/0104-6632.20170343s20150279>
- Ascher, S., Sloan, W., Watson, I., & You, S. (2022). A comprehensive artificial neural network model for gasification process prediction. *Applied Energy*, 320, 119289. <https://doi.org/10.1016/j.apenergy.2022.119289>
- Bakari, R., Kivevele, T., Huang, X., & Jande, Y. A. C. (2021). Sub- And Supercritical Water Gasification of Rice Husk: Parametric Optimization Using the I-Optimality Criterion. *ACS Omega*, 6(19), 12480–12499. <https://doi.org/10.1021/acsomega.0c06318>
- Basu, P., & Mettanan, V. (2009). Biomass Gasification in Supercritical Water -- A Review. *International Journal of Chemical Reactor Engineering*, 7(1). <https://doi.org/10.2202/1542-6580.1919>
- Beck, M. W. (2018). Visualization and Analysis Tools for Neural Networks. *Journal of Statistical Software*, 85(11). <https://doi.org/10.18637/jss.v085.i11>
- Blair, J., & Mataraarachchi, S. (2021). A Review of Landfills, Waste and the Nearly Forgotten Nexus with Climate Change. *Environments*, 8(8), 73. <https://doi.org/10.3390/environments8080073>
- Brereton, R. G. (2019). ANOVA tables and statistical significance of models. *Journal of Chemometrics*, 33(3). <https://doi.org/10.1002/cem.3019>
- Brunner, G. (2009). Near critical and supercritical water. Part I. Hydrolytic and hydrothermal processes. *The Journal of Supercritical Fluids*, 47(3), 373–381. <https://doi.org/10.1016/j.supflu.2008.09.002>
- Cao, W., Wei, W., Jin, H., Yi, L., & Wang, L. (2022). Optimize hydrogen production from chicken manure gasification in supercritical water by experimental and kinetics study. *Journal of Environmental Chemical Engineering*, 10(3), 107591. <https://doi.org/10.1016/j.jece.2022.107591>
- Chen, Y., Yi, L., Wei, W., Jin, H., & Guo, L. (2022). Hydrogen production by sewage sludge gasification in supercritical water with high heating rate batch reactor. *Energy*, 238, 121740. <https://doi.org/10.1016/j.energy.2021.121740>
- Córdoba, V. E., Mussi, J., De Paula, M., & Acosta, G. G. (2023). Prediction of Biomethane Production of Cheese Whey by Using Artificial Neural Networks. *IEEE Latin America Transactions*, 21(9), 1032–1039. <https://doi.org/10.1109/TLA.2023.10251810>
- Demirbas, A. (2011). Waste management, waste resource facilities and waste conversion processes. *Energy Conversion and Management*, 52(2), 1280–1287. <https://doi.org/10.1016/j.enconman.2010.09.025>
- DEMİRBAY, B., & KARAKULLUKÇU, A. B. (2020). Artificial Neural Network (ANN) Approach for Dynamic Viscosity of Aqueous Gelatin Solutions: A Soft Computing Study. *European Journal of Science and Technology*, 465–475. <https://doi.org/10.31590/ejosat.680773>
- Du, K.-L., Leung, C.-S., Mow, W. H., & Swamy, M. N. S. (2022). Perceptron: Learning, Generalization, Model Selection, Fault Tolerance, and Role in the Deep Learning Era. *Mathematics*, 10(24), 4730. <https://doi.org/10.3390/math10244730>
- Durakovic, B. (2017). Design of experiments application, concepts, examples: State of the art. *Periodicals of Engineering and Natural Sciences (PEN)*, 5(3). <https://doi.org/10.21533/pen.v5i3.145>
- Durgut, P. G., Tozak, M. B., & Ayvaz, M. T. (2024). SHuffled Ant Lion Optimization approach with an exponentially weighted random walk strategy. *Neural Computing and Applications*, 36(18), 10475–10499. <https://doi.org/10.1007/s00521-024-09566-5>



- Evans, S. J. (2019). How Digital Engineering and Cross-Industry Knowledge Transfer is Reducing Project Execution Risks in Oil and Gas. *Day 2 Tue, May 07, 2019*. <https://doi.org/10.4043/29458-MS>
- Farooq, M. U., Zafar, A. M., Raheem, W., Jalees, M. I., & Aly Hassan, A. (2022). Assessment of Algorithm Performance on Predicting Total Dissolved Solids Using Artificial Neural Network and Multiple Linear Regression for the Groundwater Data. *Water*, 14(13), 2002. <https://doi.org/10.3390/w14132002>
- Fozer, D., Kiss, B., Lorincz, L., Szekeley, E., Mizsey, P., & Nemeth, A. (2019). Improvement of microalgae biomass productivity and subsequent biogas yield of hydrothermal gasification via optimization of illumination. *Renewable Energy*, 138, 1262–1272. <https://doi.org/10.1016/j.renene.2018.12.122>
- Gammoudi, N., Mabrouk, M., Bouhemda, T., Nagaz, K., & Ferchichi, A. (2021). Modeling and optimization of capsaicin extraction from Capsicum annuum L. using response surface methodology (RSM), artificial neural network (ANN), and Simulink simulation. *Industrial Crops and Products*, 171, 113869. <https://doi.org/10.1016/j.indcrop.2021.113869>
- GUO, L., LU, Y., ZHANG, X., JI, C., GUAN, Y., & PEI, A. (2007). Hydrogen production by biomass gasification in supercritical water: A systematic experimental and analytical study. *Catalysis Today*, 129(3–4), 275–286. <https://doi.org/10.1016/j.cattod.2007.05.027>
- Guo, Q., & Dai, X. (2017). Analysis on carbon dioxide emission reduction during the anaerobic synergetic digestion technology of sludge and kitchen waste: Taking kitchen waste synergetic digestion project in Zhenjiang as an example. *Waste Management*, 69, 360–364. <https://doi.org/10.1016/j.wasman.2017.08.033>
- Hantoko, D., Antoni, Kanchanatip, E., Yan, M., Weng, Z., Gao, Z., & Zhong, Y. (2019). Assessment of sewage sludge gasification in supercritical water for H<sub>2</sub>-rich syngas production. *Process Safety and Environmental Protection*, 131, 63–72. <https://doi.org/10.1016/j.psep.2019.08.035>
- Hardiansyah, H. (2021). Multi-Objective Ant Lion Optimizer for Solving Environmental/Economic Dispatch. *PRZEGLĄD ELEKTROTECHNICZNY*, 1(2), 155–160. <https://doi.org/10.15199/48.2021.02.32>
- Houcinate, I., Outili, N., & Meniai, A. H. (2018). Optimization of gas production and efficiency of supercritical glycerol gasification using response surface methodology. *Biofuels*, 9(5), 625–633. <https://doi.org/10.1080/17597269.2018.1433968>
- Ibtissem, H., Nawel, O., Hassen, M. A., & Elsa, W.-H. (2019). Supercritical water gasification of glycerol for Hydrogen production using response surface methodology. *10th International Renewable Energy Congress (IREC)*, 1–6. <https://doi.org/10.1109/IREC.2019.8754520>
- Inayat, M., Sulaiman, S. A., Shahbaz, M., & Bhayo, B. A. (2020). Application of response surface methodology in catalytic co-gasification of palm wastes for bioenergy conversion using mineral catalysts. *Biomass and Bioenergy*, 132, 105418. <https://doi.org/10.1016/j.biombioe.2019.105418>
- Jin, H., Guo, L., Guo, J., Ge, Z., Cao, C., & Lu, Y. (2015). Study on gasification kinetics of hydrogen production from lignite in supercritical water. *International Journal of Hydrogen Energy*, 40(24), 7523–7529. <https://doi.org/10.1016/j.ijhydene.2014.12.095>
- Kavitha Mayilvaganan, M., & Naidu, K. B. (2011). *Application of Artificial Neural Network for the Prediction of Groundwater Level in Hard Rock Region* (pp. 673–682). [https://doi.org/10.1007/978-3-642-24043-0\\_68](https://doi.org/10.1007/978-3-642-24043-0_68)
- Kayri, M. (2016). Predictive Abilities of Bayesian Regularization and Levenberg–Marquardt Algorithms in Artificial Neural Networks: A Comparative Empirical Study on Social Data. *Mathematical and Computational Applications*, 21(2), 20. <https://doi.org/10.3390/mca2102020>
- Kemeterian LHK. (2023). *Data Timbulan Sampah Nasional*. <https://sipsn.menlhk.go.id/sipsn/public/data/timbulan>
- Khandelwal, K., Nanda, S., Boahene, P., & Dalai, A. K. (2024). Hydrogen production from supercritical water gasification of canola residues. *International Journal of Hydrogen Energy*, 49, 1518–1527. <https://doi.org/10.1016/j.ijhydene.2023.10.228>
- Kiranyaz, S., Ince, T., Iosifidis, A., & Gabbouj, M. (2017). Generalized model of biological neural networks: Progressive operational perceptrons. *2017 International Joint Conference on Neural Networks (IJCNN)*, 2477–2485. <https://doi.org/10.1109/IJCNN.2017.7966157>
- Kulkarni, S. P., Joshi, S. S., & Kulkarni, A. A. (2023). Reaction pathways and kinetics of *N*-acetyl-  $\alpha$ -D-glucosamine hydrolysis in sub- and supercritical water. *Reaction Chemistry & Engineering*, 8(5), 1097–1108. <https://doi.org/10.1039/D3RE00046J>
- Li, B., Zhang, B., Guan, Q., Chen, S., & Ning, P. (2018). Activity of Ni/CeO<sub>2</sub> catalyst for gasification of phenol in supercritical water. *International Journal of Hydrogen Energy*, 43(41), 19010–19018. <https://doi.org/10.1016/j.ijhydene.2018.08.105>
- Li, H., Lei, J., Jia, M., Xu, H., & Wu, S. (2023). High Dimensional Model Representation Approach for Prediction and Optimization of the Supercritical Water Gasification System Coupled with Photothermal Energy Storage. *Processes*, 11(8), 2313. <https://doi.org/10.3390/pr11082313>
- Li, J., Pan, L., Suvama, M., & Wang, X. (2021). Machine learning aided supercritical water gasification for H<sub>2</sub>-rich syngas production with process optimization and catalyst screening. *Chemical Engineering Journal*, 426, 131285. <https://doi.org/10.1016/j.cej.2021.131285>
- Li, L., Li, X., & Cao, W. (2023). Reaction pathway and kinetics study on supercritical water gasification of oily sludge. *Journal of Analytical and Applied Pyrolysis*, 170, 105920. <https://doi.org/10.1016/j.jaap.2023.105920>
- Lin, R., Zhou, Z., You, S., Rao, R., & Kuo, C.-C. J. (2024). Geometrical Interpretation and Design of Multilayer Perceptrons. *IEEE Transactions on Neural Networks and Learning Systems*, 35(2), 2545–2559. <https://doi.org/10.1109/TNNLS.2022.3190364>
- Lombardi, L., Carnevale, E., & Corti, A. (2015). A review of technologies and performances of thermal treatment systems for energy recovery from waste. *Waste Management*, 37, 26–44. <https://doi.org/10.1016/j.wasman.2014.11.010>
- Lu, P., Huang, Q., Boursalas, A. C. (Thanos), Themelis, N. J., Chi, Y., & Yan, J. (2019). Review on fate of chlorine during thermal processing of solid wastes. *Journal of Environmental Sciences (China)*, 78, 13–28. Chinese Academy of Sciences. <https://doi.org/10.1016/j.jes.2018.09.003>
- Mirjalili, S. (2015). The Ant Lion Optimizer. *Advances in Engineering Software*, 83, 80–98. <https://doi.org/10.1016/j.advengsoft.2015.01.010>
- Mirjalili, S., Jangir, P., & Saremi, S. (2017). Multi-objective ant lion optimizer: a multi-objective optimization algorithm for solving engineering problems. *Applied Intelligence*, 46(1), 79–95. <https://doi.org/10.1007/s10489-016-0825-8>
- Mondal, P. (2022). From municipal solid waste (MSW) to hydrogen: Performance optimization of a fixed bed gasifier using Box-Benken method. *International Journal of Hydrogen Energy*, 47(46), 20064–20075. <https://doi.org/10.1016/j.ijhydene.2022.04.150>
- Nanda, S., Reddy, S. N., Vo, D. N., Sahoo, B. N., & Kozinski, J. A. (2018). Catalytic gasification of wheat straw in hot compressed (subcritical and supercritical) water for hydrogen production. *Energy Science & Engineering*, 6(5), 448–459. <https://doi.org/10.1002/ese3.219>
- Okolie, J. A., Nanda, S., Dalai, A. K., & Kozinski, J. A. (2020). Optimization and modeling of process parameters during hydrothermal gasification of biomass model compounds to generate hydrogen-rich gas products. *International Journal of Hydrogen Energy*, 45(36), 18275–18288. <https://doi.org/10.1016/j.ijhydene.2019.05.132>
- Pandey, D. S., Das, S., Pan, I., Leahy, J. J., & Kwapinski, W. (2016). Artificial neural network based modelling approach for municipal solid waste gasification in a fluidized bed reactor. *Waste Management*, 58, 202–213. <https://doi.org/10.1016/j.wasman.2016.08.023>
- Pandey, D. S., Pan, I., Das, S., Leahy, J. J., & Kwapinski, W. (2015). Multi-gene genetic programming based predictive models for municipal solid waste gasification in a fluidized bed gasifier. *Bioresour Technol*, 179, 524–533. <https://doi.org/10.1016/j.biortech.2014.12.048>
- Popoola, S. I., Jefia, A., Atayero, A. A., Kingsley, O., Faruk, N., Oseni, O. F., & Abolade, R. O. (2019). Determination of Neural Network Parameters for Path Loss Prediction in Very High Frequency Wireless Channel. *IEEE Access*, 7, 150462–150483. <https://doi.org/10.1109/ACCESS.2019.2947009>
- Puig-Arnau, M., Hernández, J. A., Bruno, J. C., & Coronas, A. (2013). Artificial neural network models for biomass gasification in fluidized bed gasifiers. *Biomass and Bioenergy*, 49, 279–289. <https://doi.org/10.1016/j.biombioe.2012.12.012>

- Qian, J., Wang, T., Jiang, H., Yu, Y., & Miao, D. (2023). A TOPSIS method based on sequential three-way decision. *Applied Intelligence*, 53(24), 30661–30676. <https://doi.org/10.1007/s10489-023-05183-2>
- Qiao, X., Ding, J., She, C., Mao, W., Zhang, A., Feng, B., & Xu, Y. (2024). A metaheuristic Multi-Objective optimization of energy and environmental performances of a Waste-to-Energy system based on waste gasification using particle swarm optimization. *Energy Conversion and Management*, 317. <https://doi.org/10.1016/j.enconman.2024.118844>
- Qiu, Y., Liu, Y., Fang, C., Ju, M., Xia, R., & Wang, Y. (2024). Supercritical water gasification of oily sludge and its life cycle assessment. *BioResources*, 19(2), 2327–2341. <https://doi.org/10.15376/biores.19.2.2327-2341>
- Ramaswamy, M. D. K., Thangarasu, V., Jaganathan, V. M., Angkayarkan Vinayakaselvi, M., & Ramanathan, A. (2025). Synthesis, characterization and optimization of gasification products from Aegle Marmelos Correa shell in a downdraft gasifier using ANN and RSM. *Proceedings of the Institution of Mechanical Engineers, Part E: Journal of Process Mechanical Engineering*, 239(2), 601–615. <https://doi.org/10.1177/09544089231171030>
- Rawat, S., Wagadre, L., & Kumar, S. (2024). Multi-objective genetic algorithm approach for enhanced cumulative hydrogen and methane-rich syngas emission through co-pyrolysis of de-oiled microalgae and coal blending. *Renewable Energy*, 225, 120264. <https://doi.org/10.1016/j.renene.2024.120264>
- Reddy, S. N., Nanda, S., Dalai, A. K., & Kozinski, J. A. (2014). Supercritical water gasification of biomass for hydrogen production. *International Journal of Hydrogen Energy*, 39(13), 6912–6926. <https://doi.org/10.1016/j.ijhydene.2014.02.125>
- Rizal, R., Wahyuni, F., Julian, J., Nasruddin, & Yulia, F. (2024). Optimal design and modelling of sustainable bio-catalytic enzyme for wastewater treatment using response surface methodology and artificial neural network. *Energy Sources, Part A: Recovery, Utilization, and Environmental Effects*, 46(1), 5254–5273. <https://doi.org/10.1080/15567036.2024.2332468>
- Rodriguez Correa, C., & Kruse, A. (2018). Supercritical water gasification of biomass for hydrogen production – Review. *The Journal of Supercritical Fluids*, 133, 573–590. <https://doi.org/10.1016/j.supflu.2017.09.019>
- Sesotyo, P. A., Nur, M., & Suseno, J. E. (2019). Plasma gasification modeling of municipal solid waste from Jatibarang Landfill in Semarang, Indonesia: analyzing its performance parameters for energy potential. *E3S Web of Conferences*, 14009–14015. <https://doi.org/10.1051/e3sconf/201>
- Shahbaz, M., Yusup, S., Inayat, A., Patrick, D. O., Pratama, A., & Ammar, M. (2017). Optimization of hydrogen and syngas production from PKS gasification by using coal bottom ash. *Bioresource Technology*, 241, 284–295. <https://doi.org/10.1016/j.biortech.2017.05.119>
- Shen, L., Liu, S., Fu, S., Wang, Y., Zhou, W., & Bai, B. (2025). Thermodynamic analysis and multi-criteria optimization of supercritical water gasification for polygeneration of hydrogen, heat, and electricity from plastic wastes. *International Journal of Hydrogen Energy*, 100, 284–295. <https://doi.org/10.1016/j.ijhydene.2024.12.345>
- Shih, H.-S. (2022). *TOPSIS Basics* (pp. 17–31). [https://doi.org/10.1007/978-3-031-09577-1\\_2](https://doi.org/10.1007/978-3-031-09577-1_2)
- Soesanti, I., & Syahputra, R. (2022). Multiobjective Ant Lion Optimization for Performance Improvement of Modern Distribution Network. *IEEE Access*, 10, 12753–12773. <https://doi.org/10.1109/ACCESS.2022.3147366>
- Su, H., Kanchanatip, E., Wang, D., Zheng, R., Huang, Z., Chen, Y., Mubeen, I., & Yan, M. (2020). Production of H<sub>2</sub>-rich syngas from gasification of unsorted food waste in supercritical water. *Waste Management*, 102, 520–527. <https://doi.org/10.1016/j.wasman.2019.11.018>
- Su, W., Cai, C., Liu, P., Lin, W., Liang, B., Zhang, H., Ma, Z., Ma, H., Xing, Y., & Liu, W. (2020). Supercritical water gasification of food waste: Effect of parameters on hydrogen production. *International Journal of Hydrogen Energy*, 45(29), 14744–14755. <https://doi.org/10.1016/j.ijhydene.2020.03.190>
- Sun, J., Zhang, R., Wang, M., Zhang, J., Qiu, S., Tian, W., & Su, G. H. (2022). Multi-objective optimization of helical coil steam generator in high temperature gas reactors with genetic algorithm and response surface method. *Energy*, 259, 124976. <https://doi.org/10.1016/j.energy.2022.124976>
- Umar, H. A., Shaik, N. B., Inayat, M., & Sulaiman, S. A. (2024). ANN-RSM based multi-parametric optimisation and modelling of H<sub>2</sub> and syngas from co-gasification of residues from oil palm plants. *Process Safety and Environmental Protection*, 188, 759–780. <https://doi.org/10.1016/j.psep.2024.05.103>
- Yadav, S. K., Joseph, D., & Jigeesh, N. (2018). A review on industrial applications of TOPSIS approach. *International Journal of Services and Operations Management*, 30(1), 23. <https://doi.org/10.1504/IJSOM.2018.091438>
- Yadav, V., Karmakar, S., Kalbar, P. P., & Dikshit, A. K. (2019). PyTOPS: A Python based tool for TOPSIS. *SoftwareX*, 9, 217–222. <https://doi.org/10.1016/j.softx.2019.02.004>
- Yan, M., Su, H., Hantoko, D., Kanchanatip, E., Shahul Hamid, F. B., Zhang, S., Wang, G., & Xu, Z. (2019). Experimental study on the energy conversion of food waste via supercritical water gasification: Improvement of hydrogen production. *International Journal of Hydrogen Energy*, 44(10), 4664–4673. <https://doi.org/10.1016/j.ijhydene.2018.12.193>
- Yang, C., Wang, S., Li, Y., Zhang, Y., & Cui, C. (2021). Thermodynamic analysis of hydrogen production via supercritical water gasification of coal, sewage sludge, microalga, and sawdust. *International Journal of Hydrogen Energy*, 46(34), 18042–18050. <https://doi.org/10.1016/j.ijhydene.2020.06.198>
- Yang, Y., Zhao, L., Zhang, J., & Huang, R. (2022). Operating parametric analysis and kinetic modeling of methanol gasification in supercritical water. *The Journal of Supercritical Fluids*, 180, 105448. <https://doi.org/10.1016/j.supflu.2021.105448>
- Zaman, S. A., Roy, D., & Ghosh, S. (2020). Process modeling and optimization for biomass steam-gasification employing response surface methodology. *Biomass and Bioenergy*, 143, 105847. <https://doi.org/10.1016/j.biombioe.2020.105847>
- Zandifar, A., Esmaeilzadeh, F., & Rodríguez-Mirasol, J. (2024). Hydrogen-rich gas production via supercritical water gasification (SCWG) of oily sludge over waste tire-derived activated carbon impregnated with Ni: Characterization and optimization of activated carbon production. *Environmental Pollution*, 342. <https://doi.org/10.1016/j.envpol.2023.123078>
- Zhang, Y., Li, L., Xu, P., Liu, B., Shuai, Y., & Li, B. (2019). Hydrogen production through biomass gasification in supercritical water: A review from exergy aspect. *International Journal of Hydrogen Energy*, 44(30), 15727–15736. <https://doi.org/10.1016/j.ijhydene.2019.01.151>
- Zhao, L., Zhou, H., Yin, Y., Lu, Q., & Zhang, J. (2020). Effects of potassium carbonate on acetaldehyde gasification in supercritical water. *Energy Sources, Part A: Recovery, Utilization, and Environmental Effects*, 42(10), 1286–1298. <https://doi.org/10.1080/15567036.2019.1648602>
- Zhu, L., Li, H., Chen, S., Tian, X., Kang, X., Jiang, X., & Qiu, S. (2020). Optimization analysis of a segmented thermoelectric generator based on genetic algorithm. *Renewable Energy*, 156, 710–718. <https://doi.org/10.1016/j.renene.2020.04.120>
- Ziraba, A. K., Haregu, T. N., & Mberu, B. (2016). A review and framework for understanding the potential impact of poor solid waste management on health in developing countries. *Archives of Public Health*, 74(1), 55. <https://doi.org/10.1186/s13690-016-0166-4>

